Electronic Supplementary Information (ESI)

Heterobimetallic copper(I) complexes bearing both 1,1′-bis(diphenyl phosphino)ferrocene and functionalized 3-(2′-pyridyl)-1,2,4-triazole

Jing-Lin Chen,*[,a,d] Xue-Hua Zeng,[a] Paramaguru Ganesan,[b] Li-Hua He,[a] Jin-Sheng Liao,[a] Sui-Jun Liu,[a] He-Rui Wen,[a] Feng Zhao*[,c] and Yun Chi*[,b]

[a] *School of Metallurgy and Chemical Engineering, Jiangxi University of Science and Technology, Ganzhou 341000, People's Republic of China*

[b] *Department of Chemistry and Low Carbon Energy Research Center, National Tsing Hua University, Hsinchu 30013, Taiwan*

[c] *School of Chemistry and Chemical Engineering, Jiangxi Science and Technology Normal University, Nanchang 330013, People's Republic of China*

[d] *State Key Laboratory of Structural Chemistry, Fujian Institute of Research on the Structure of Matter, Chinese Academy of Sciences, Fuzhou 350002, People's Republic of China*

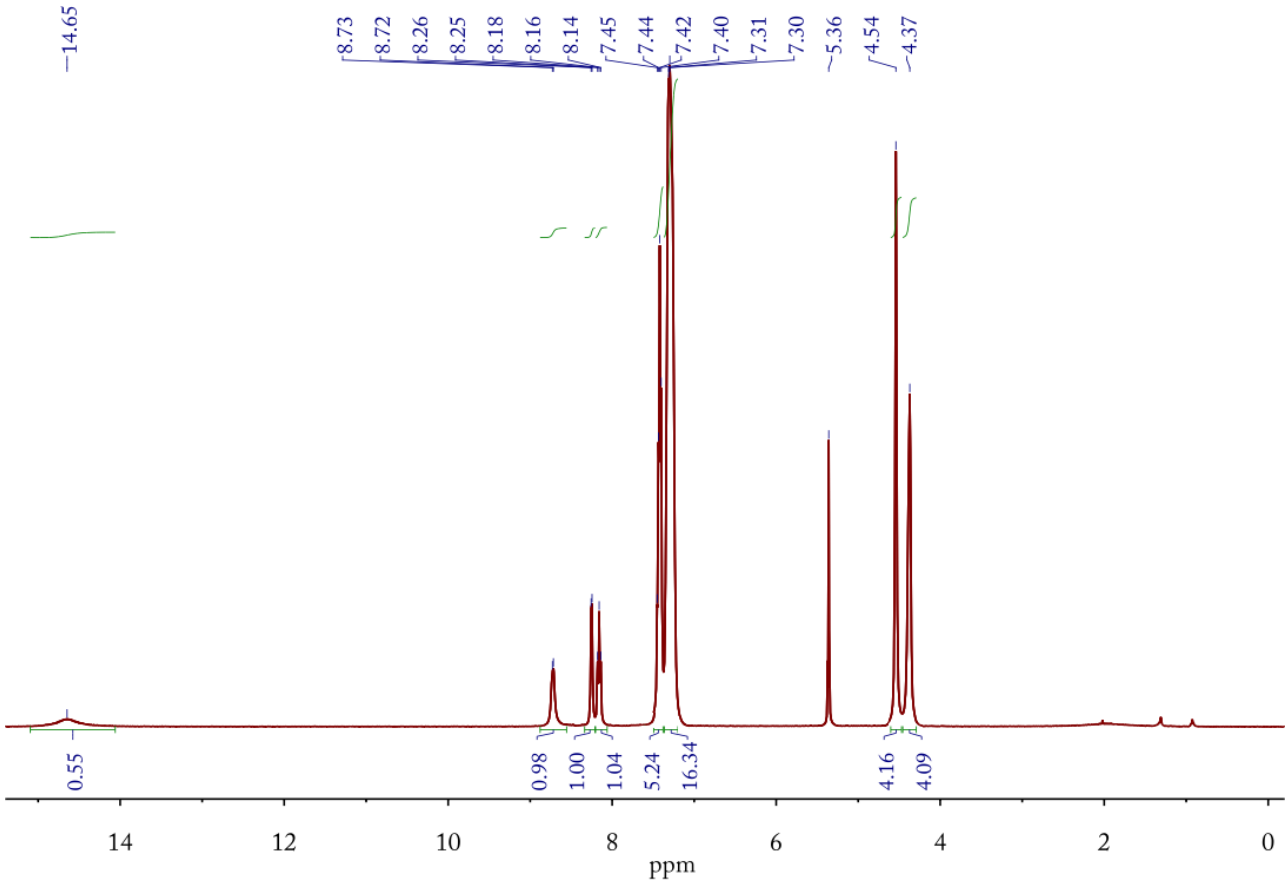

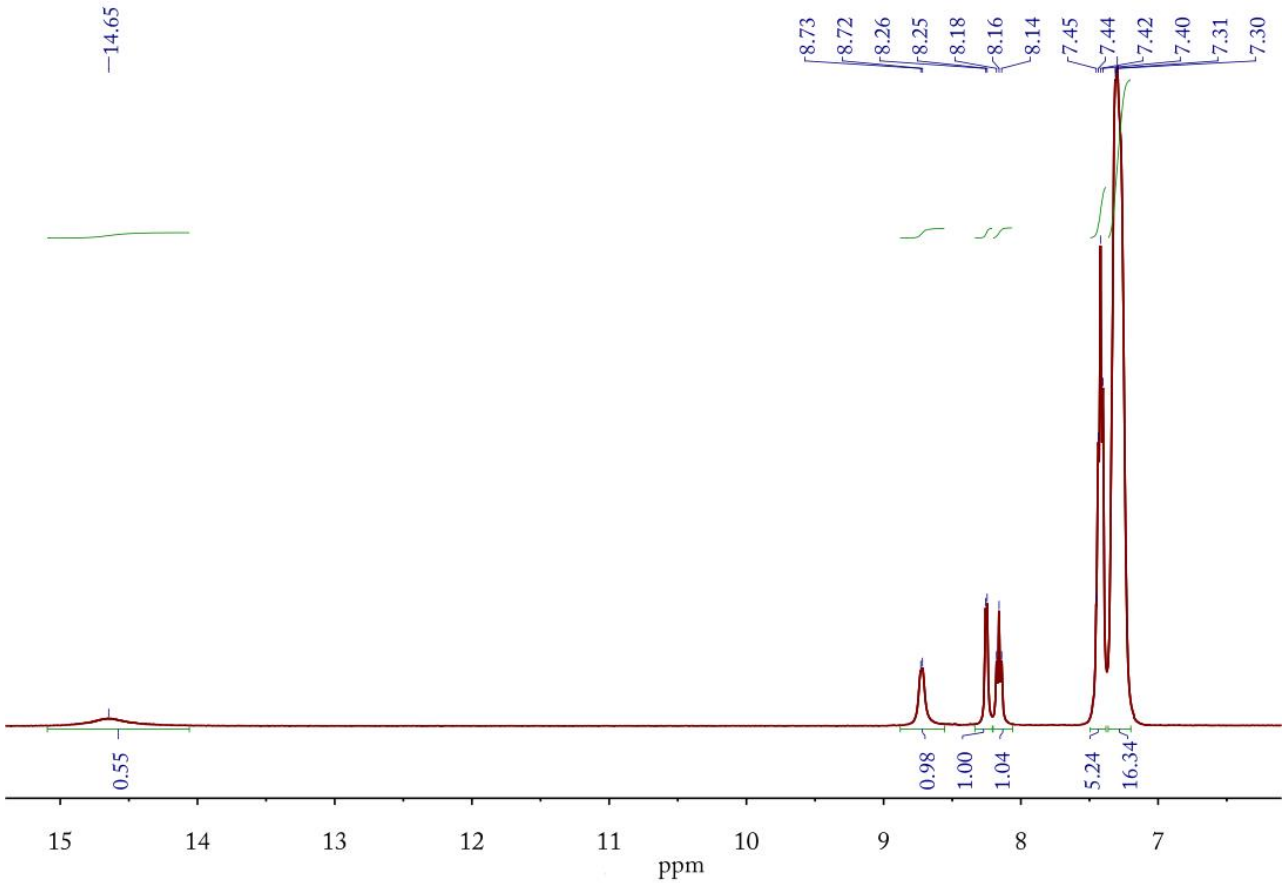

Fig. S1 ^{1}H NMR spectrum of **1** in CD_2Cl_2 at room temperature

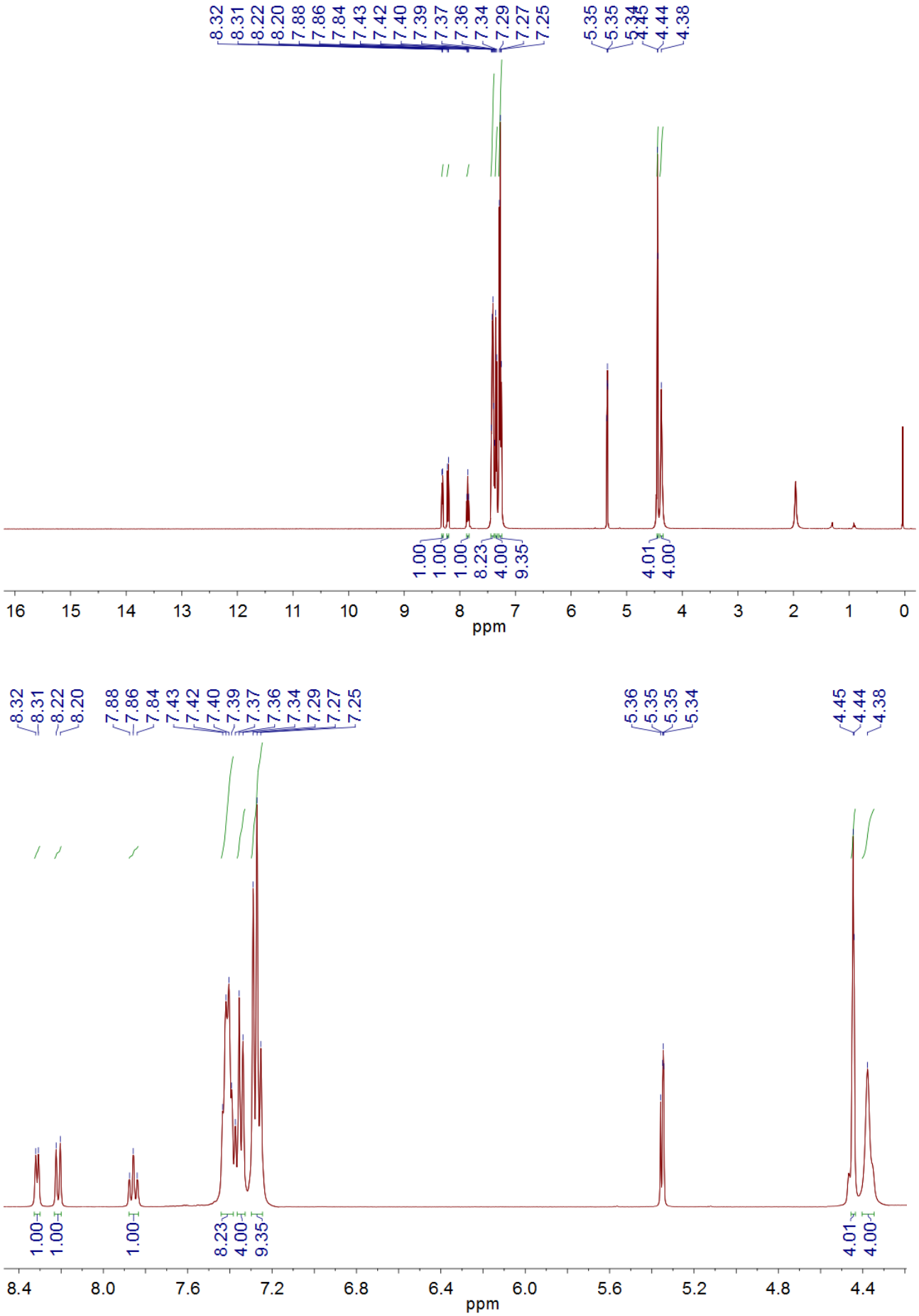

Fig. S2 ^{1}H NMR spectrum of **2** in CD_2Cl_2 at room temperature

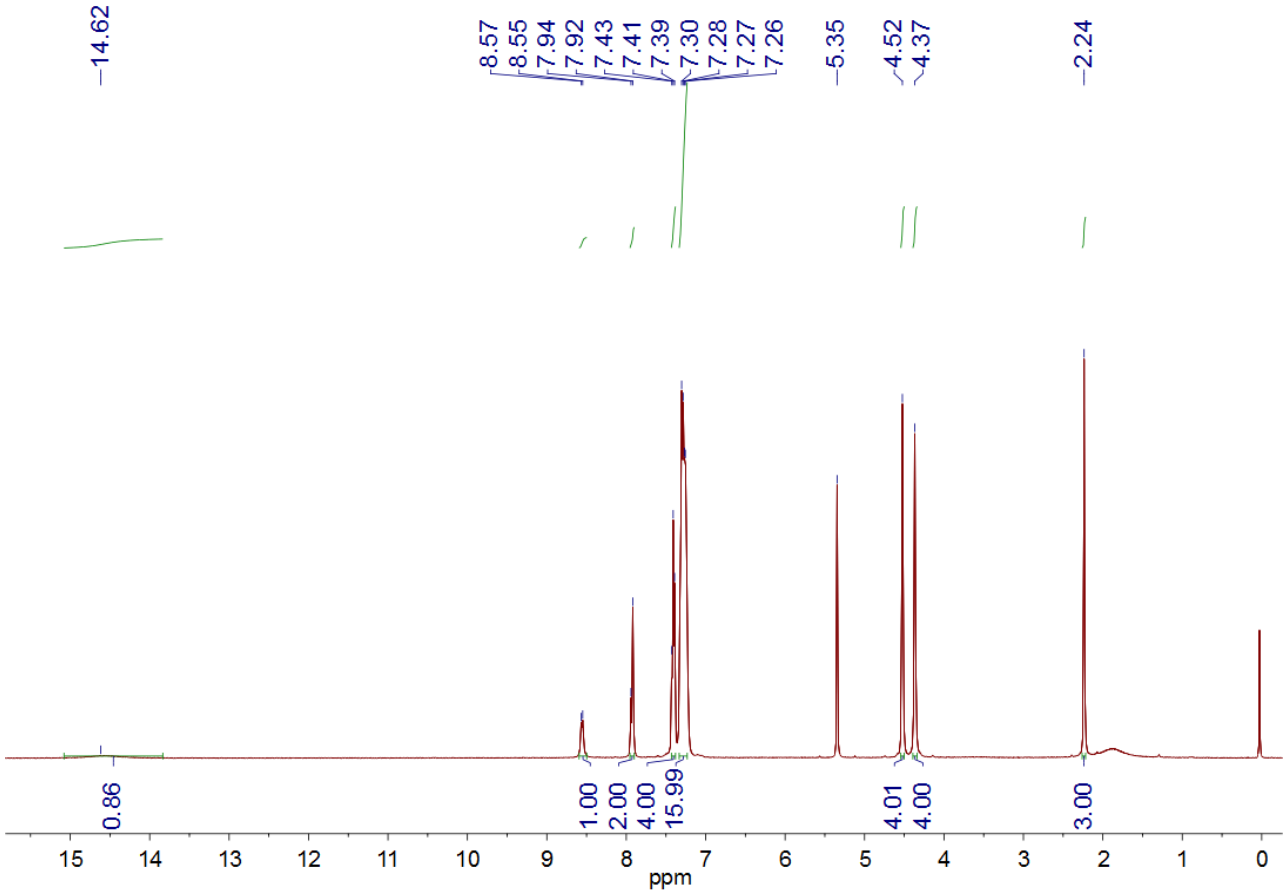

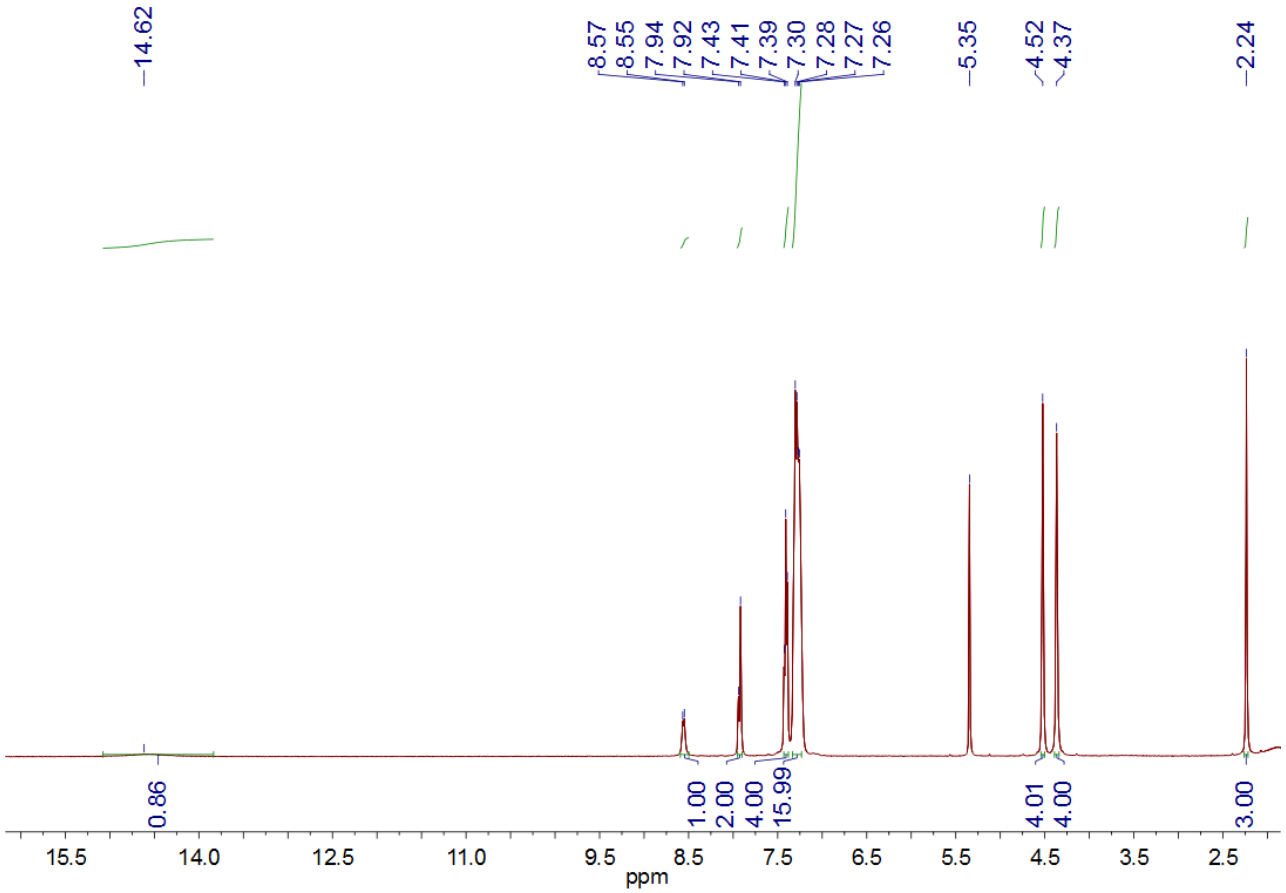

Fig. S3 ^{1}H NMR spectrum of **3** in CD_2Cl_2 at room temperature

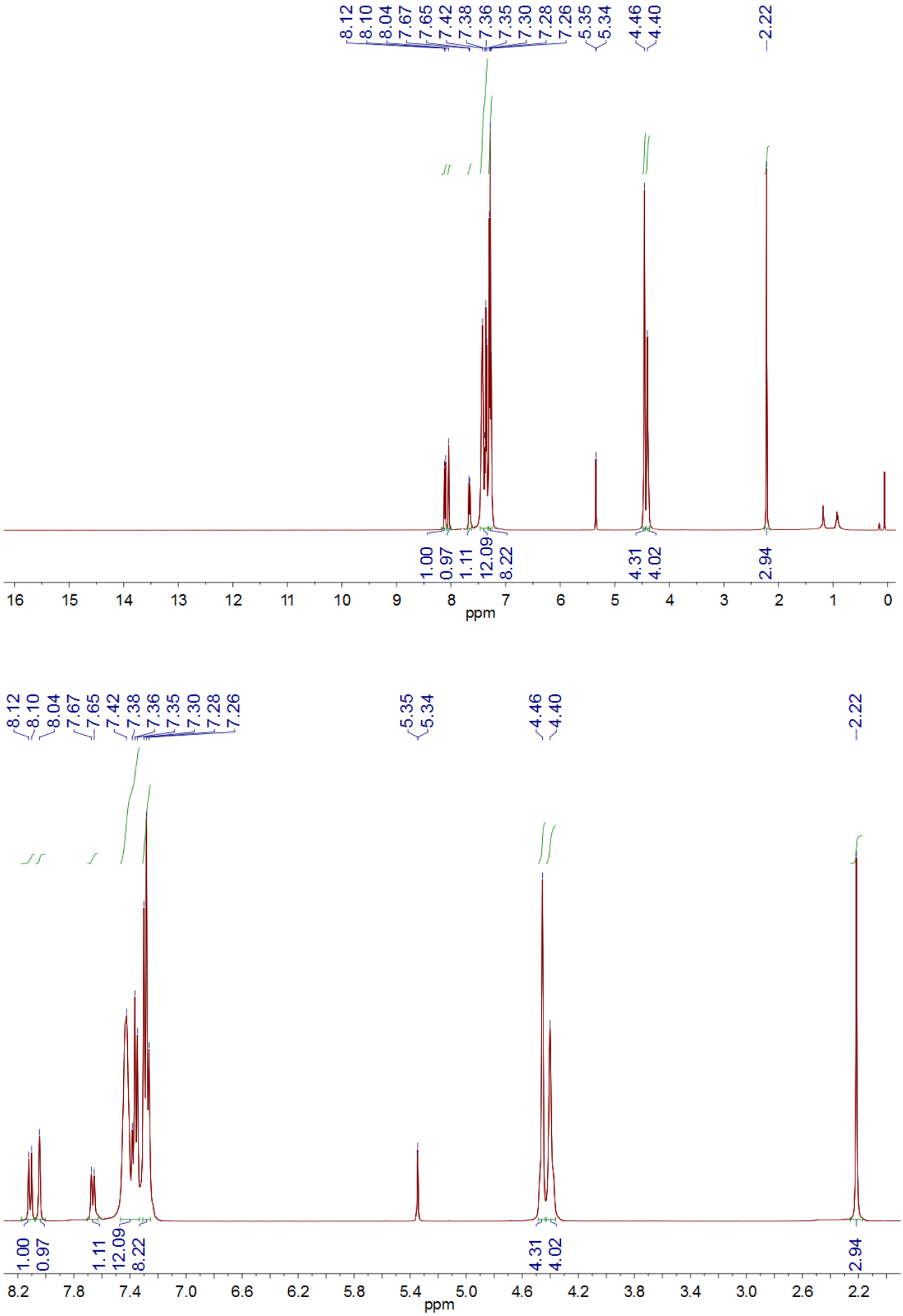

Fig. S4 ^{1}H NMR spectrum of **4** in CD_2Cl_2 at room temperature

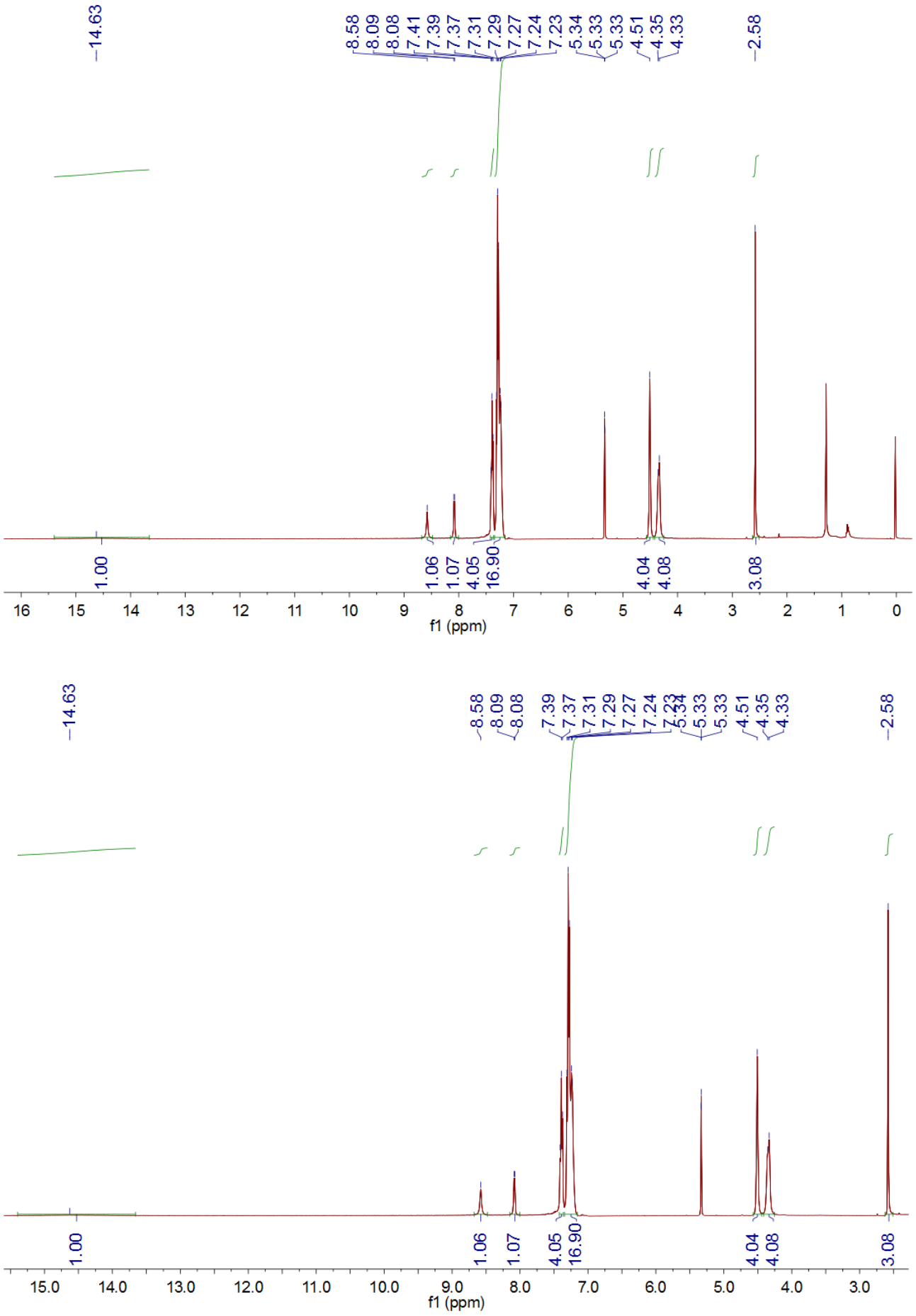

Fig. S5 ^{1}H NMR spectrum of **5** in CD_2Cl_2 at room temperature

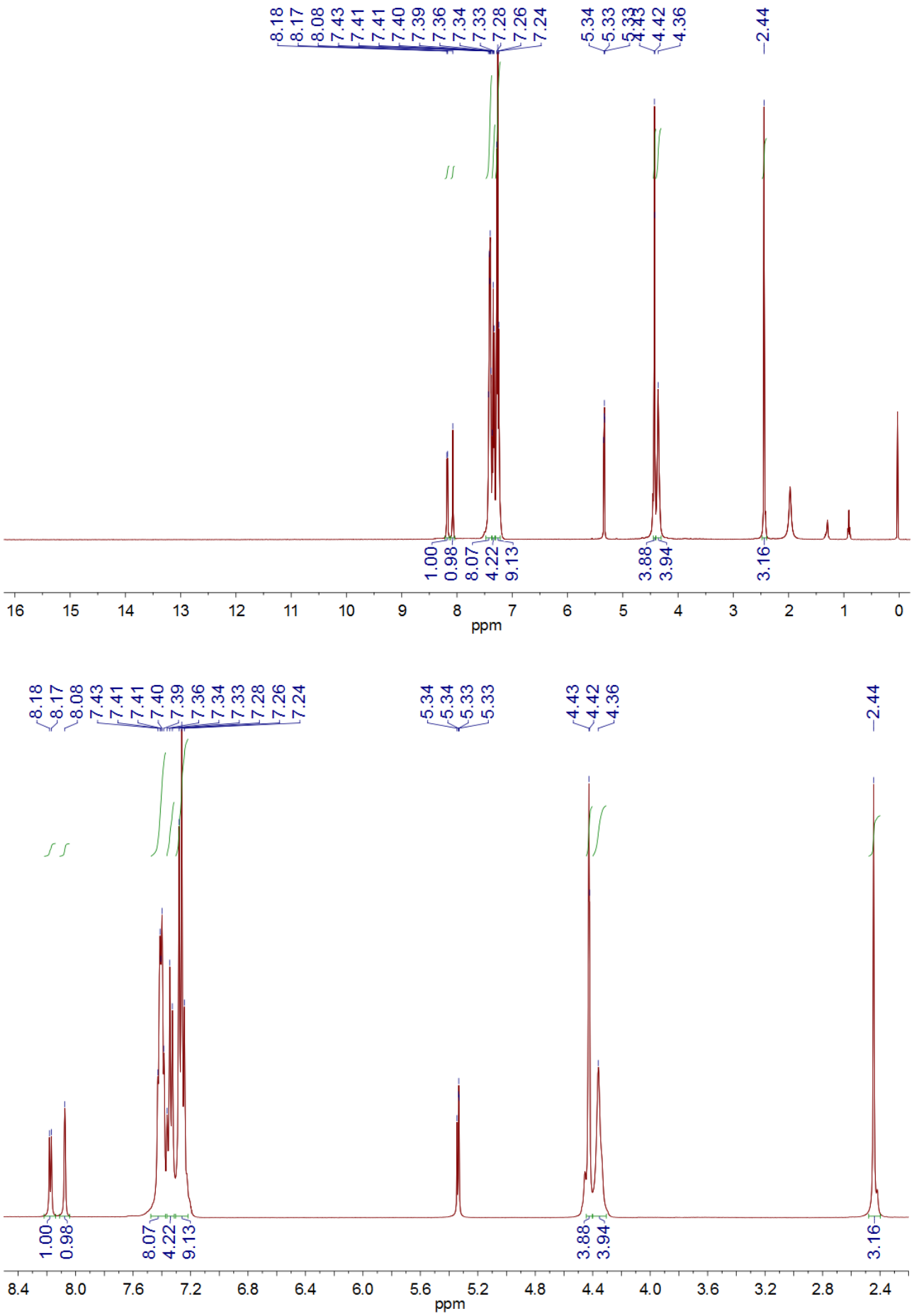

Fig. S6 ^{1}H NMR spectrum of **6** in CD_2Cl_2 at room temperature

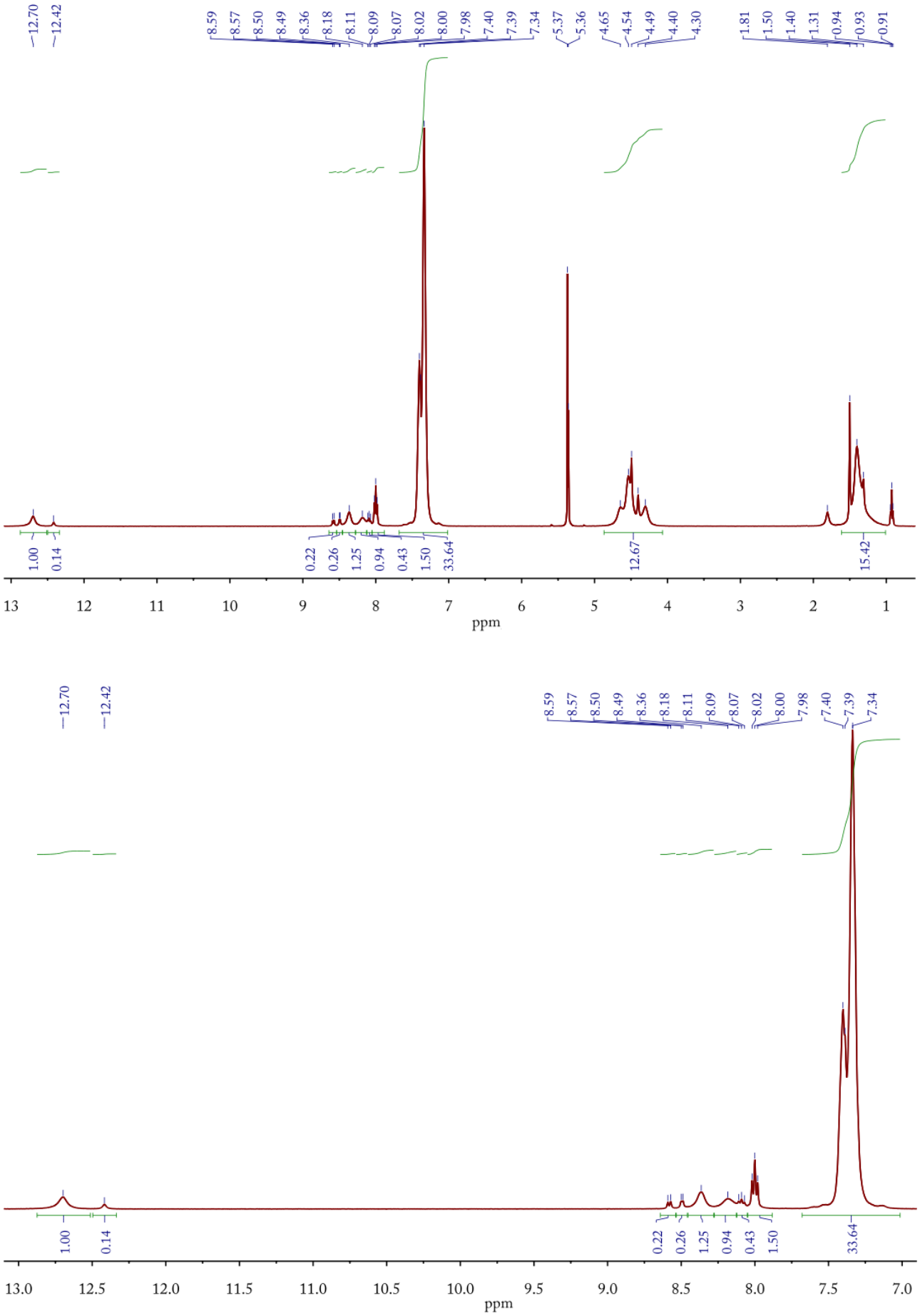

Fig. S7 ^{1}H NMR spectrum of **7** in CD_2Cl_2 at room temperature

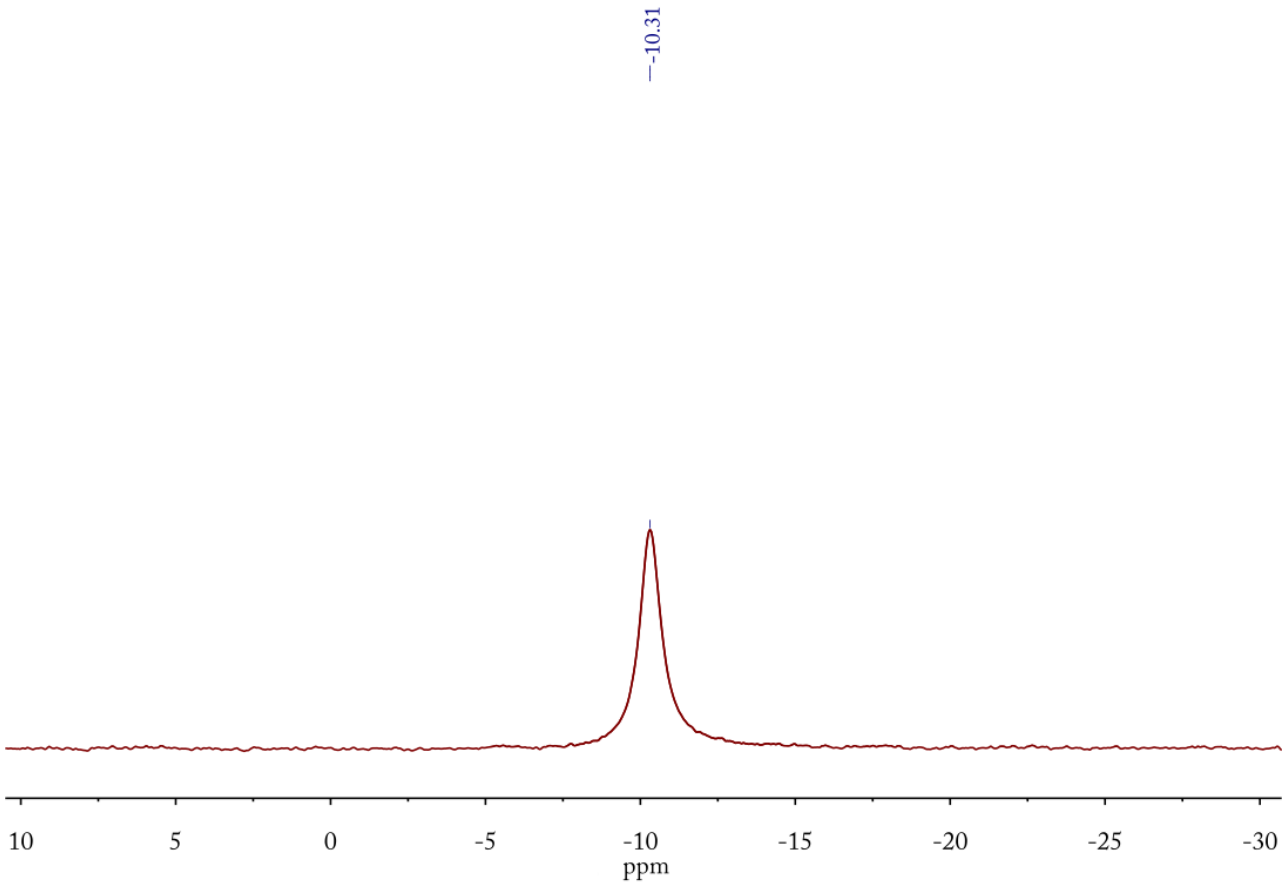

Fig. S8 ^{31}P NMR spectrum of **1** in CD_2Cl_2 at room temperature

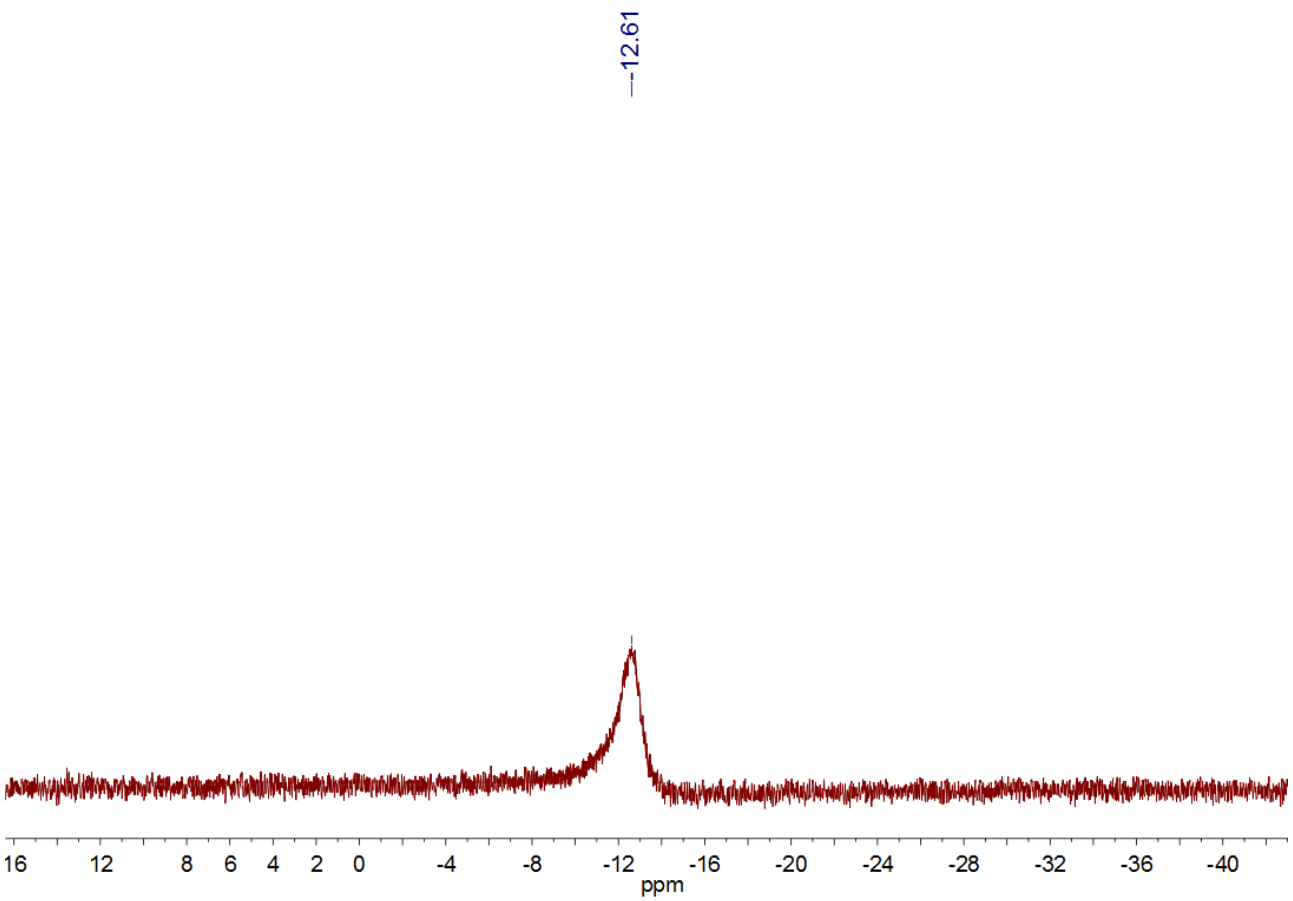

Fig. S9 ^{31}P NMR spectrum of **2** in CD_2Cl_2 at room temperature

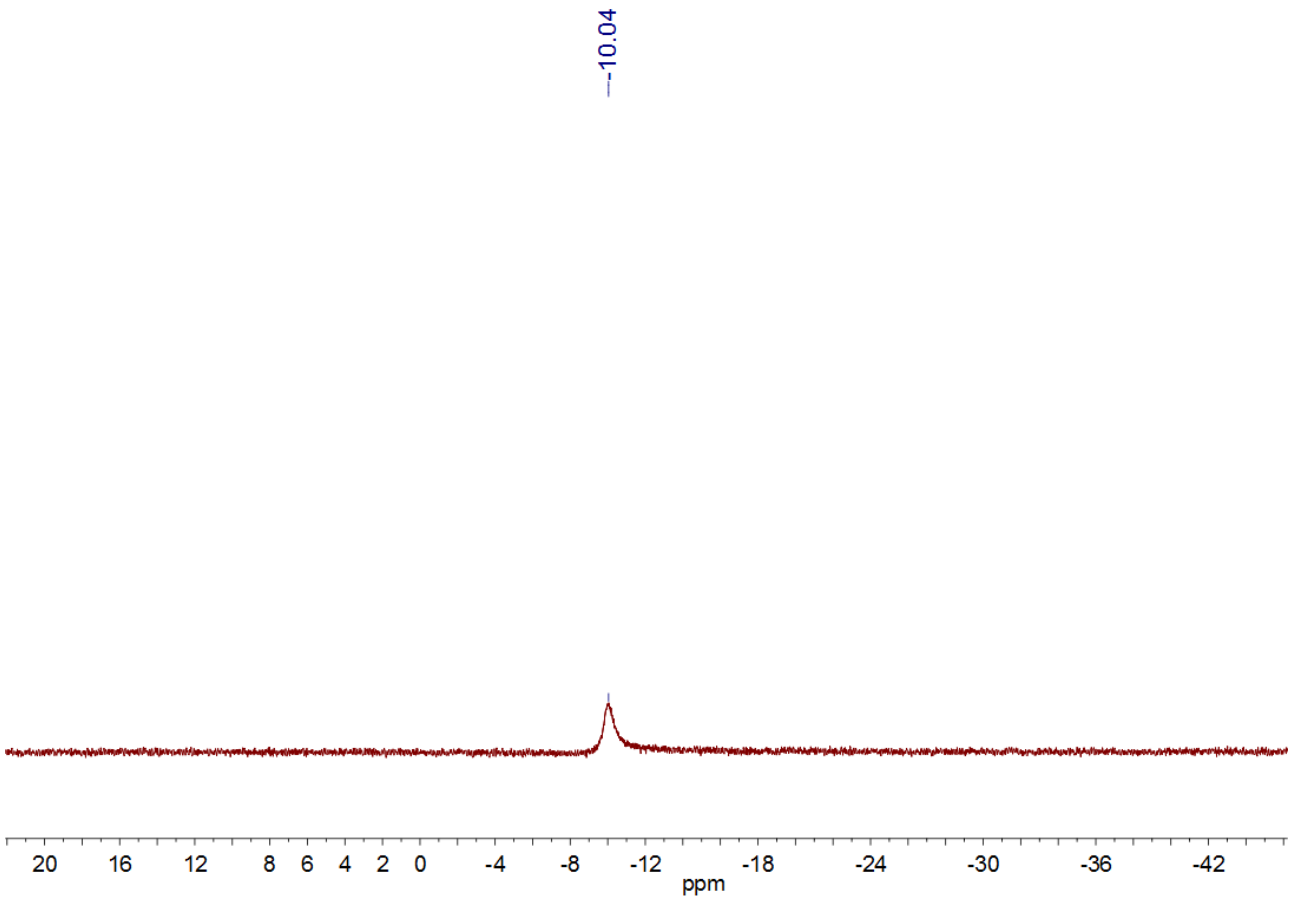

Fig. S10 ^{31}P NMR spectrum of **3** in CD_2Cl_2 at room temperature

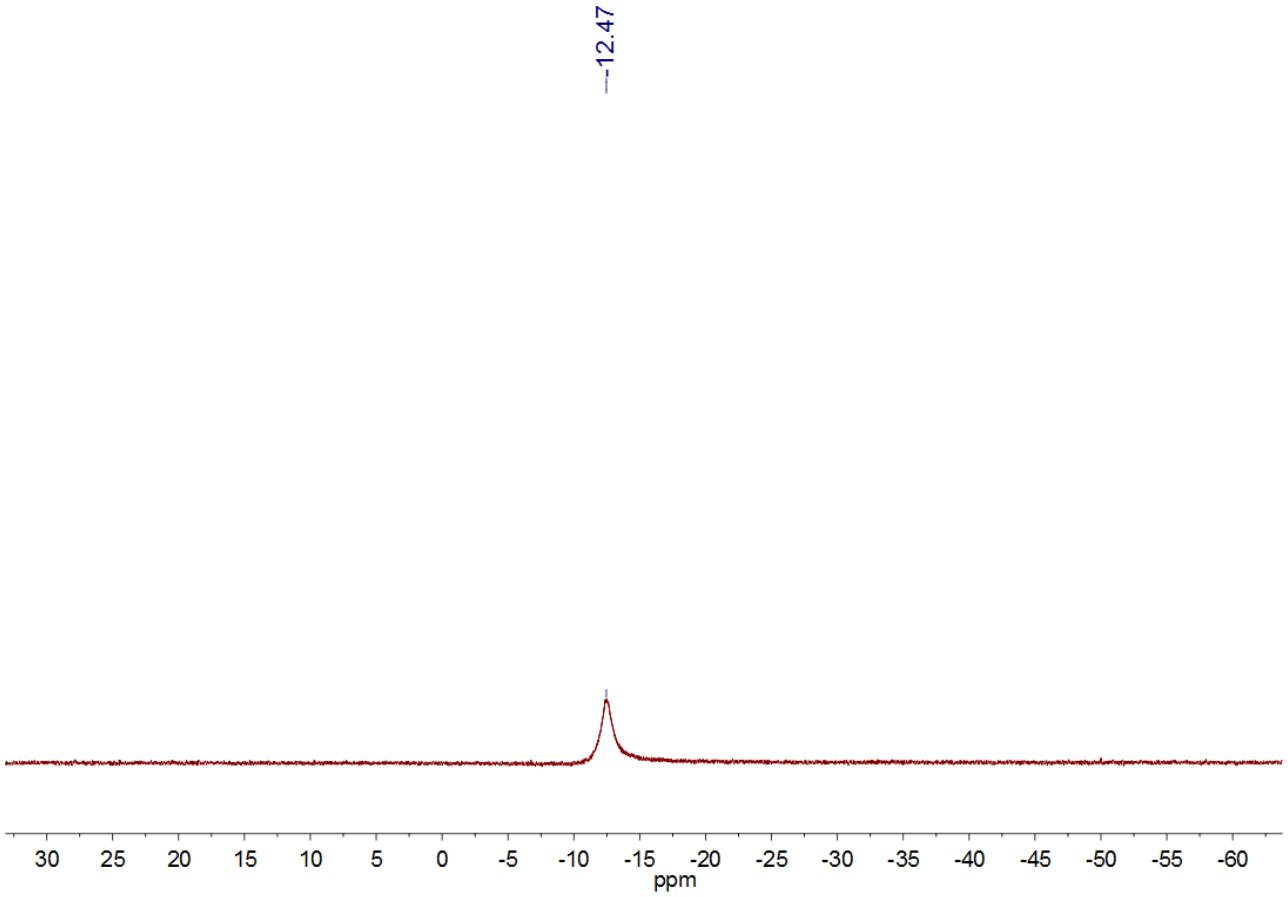

Fig. S11 ^{31}P NMR spectrum of **4** in CD_2Cl_2 at room temperature

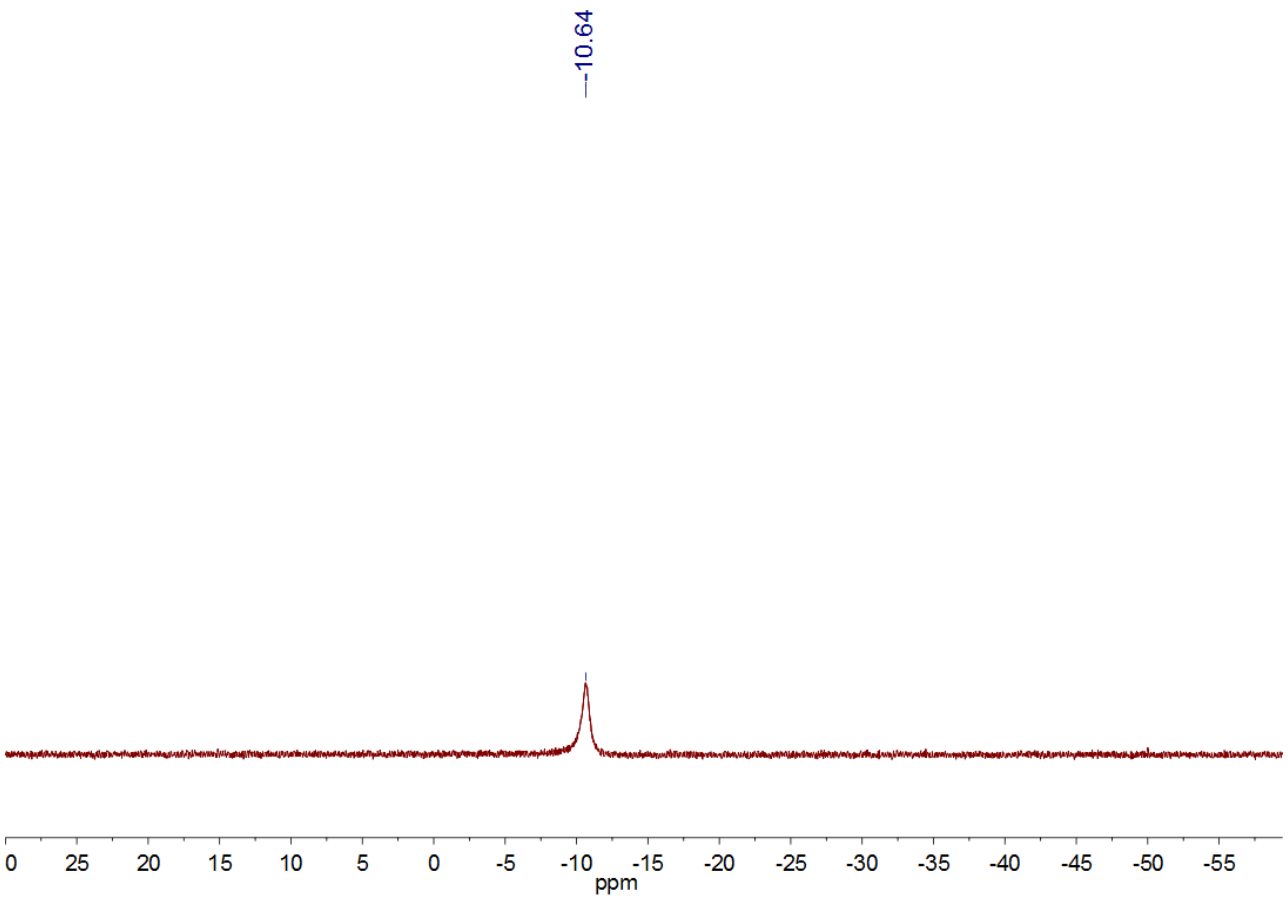

Fig. S12 ^{31}P NMR spectrum of **5** in CD_2Cl_2 at room temperature

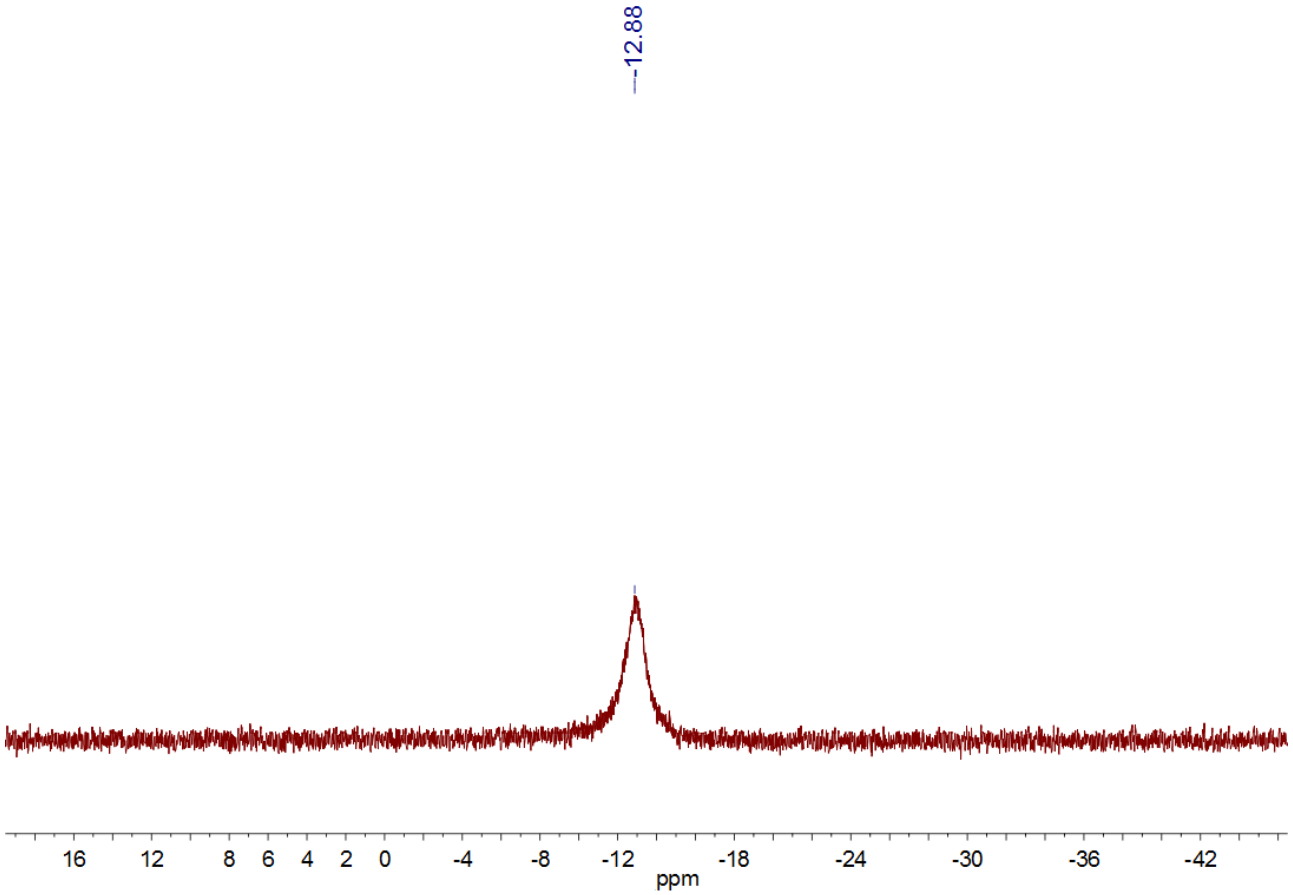

Fig. S13 ^{31}P NMR spectrum of **6** in CD_2Cl_2 at room temperature

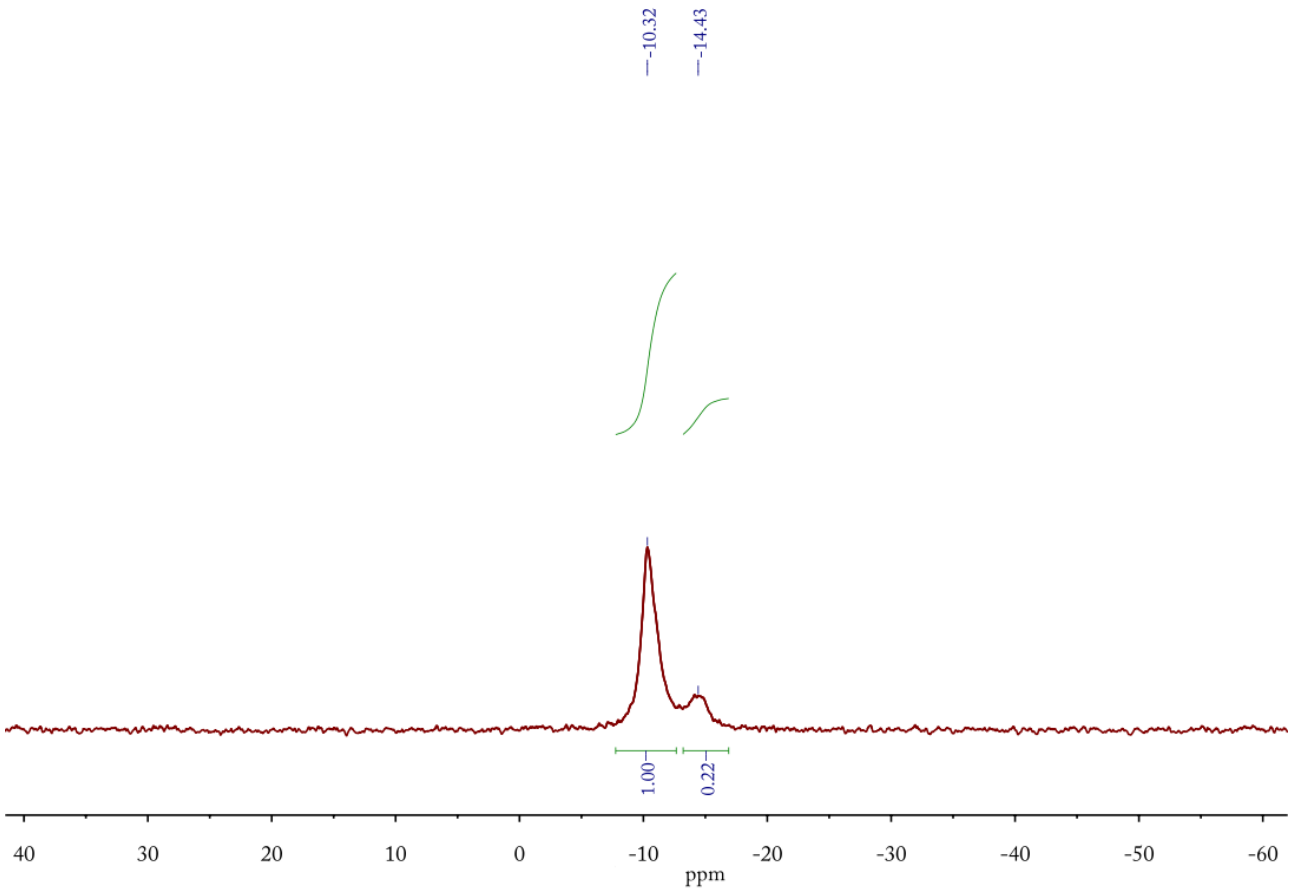

Fig. S14 ^{31}P NMR spectrum of **7** in CD_2Cl_2 at room temperature

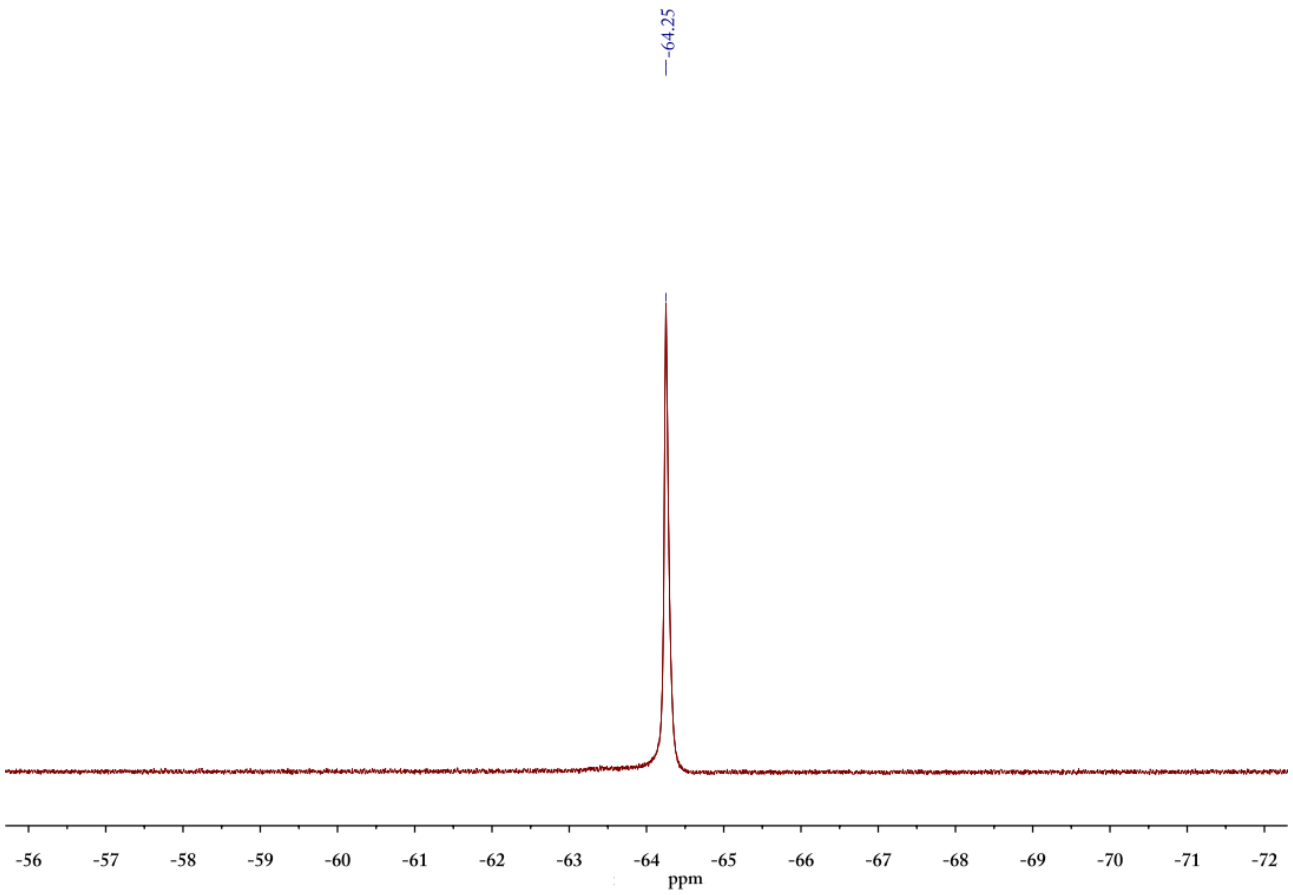

Fig. S15 ^{19}F NMR spectrum of **1** in $CDCl_3$ at room temperature

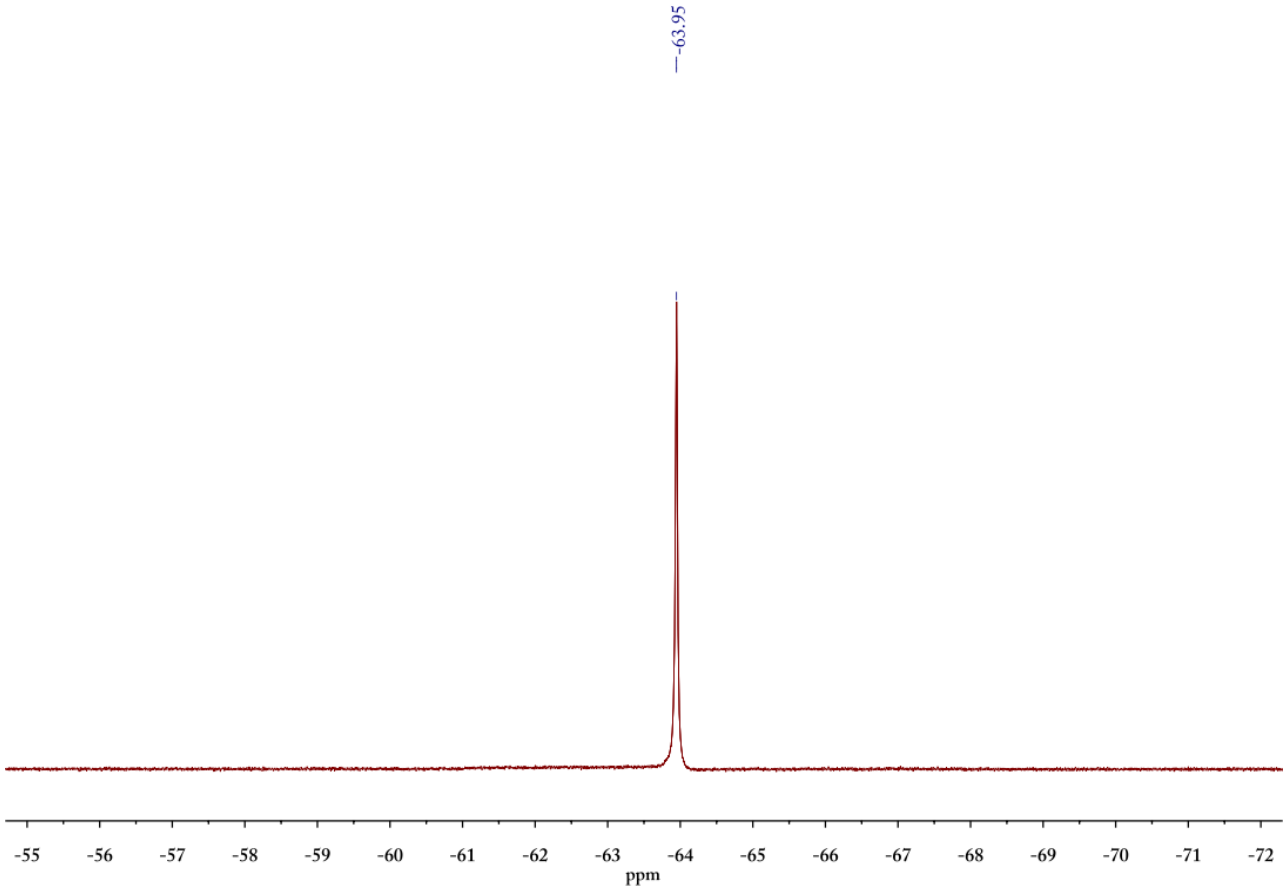

Fig. S16 ^{19}F NMR spectrum of **2** in $CDCl_3$ at room temperature

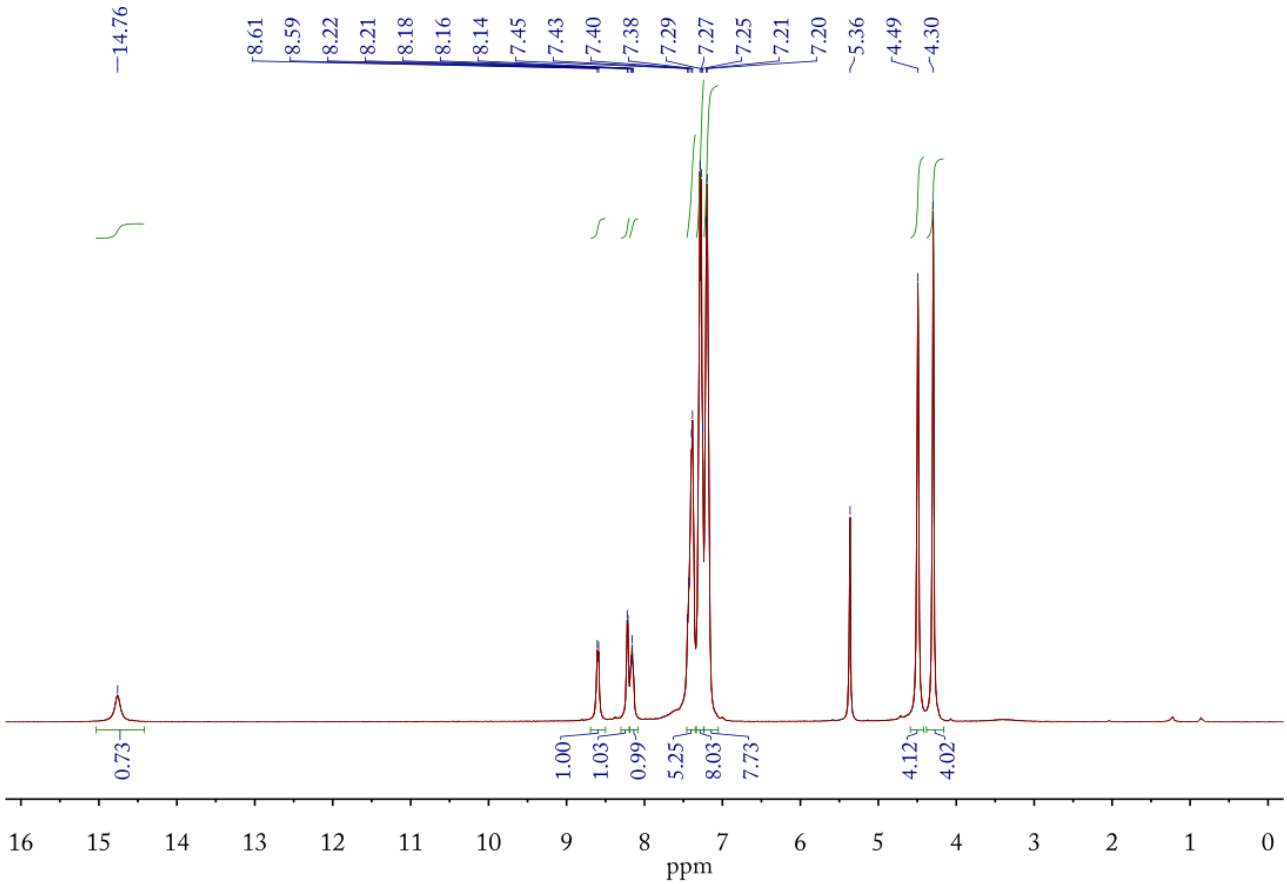

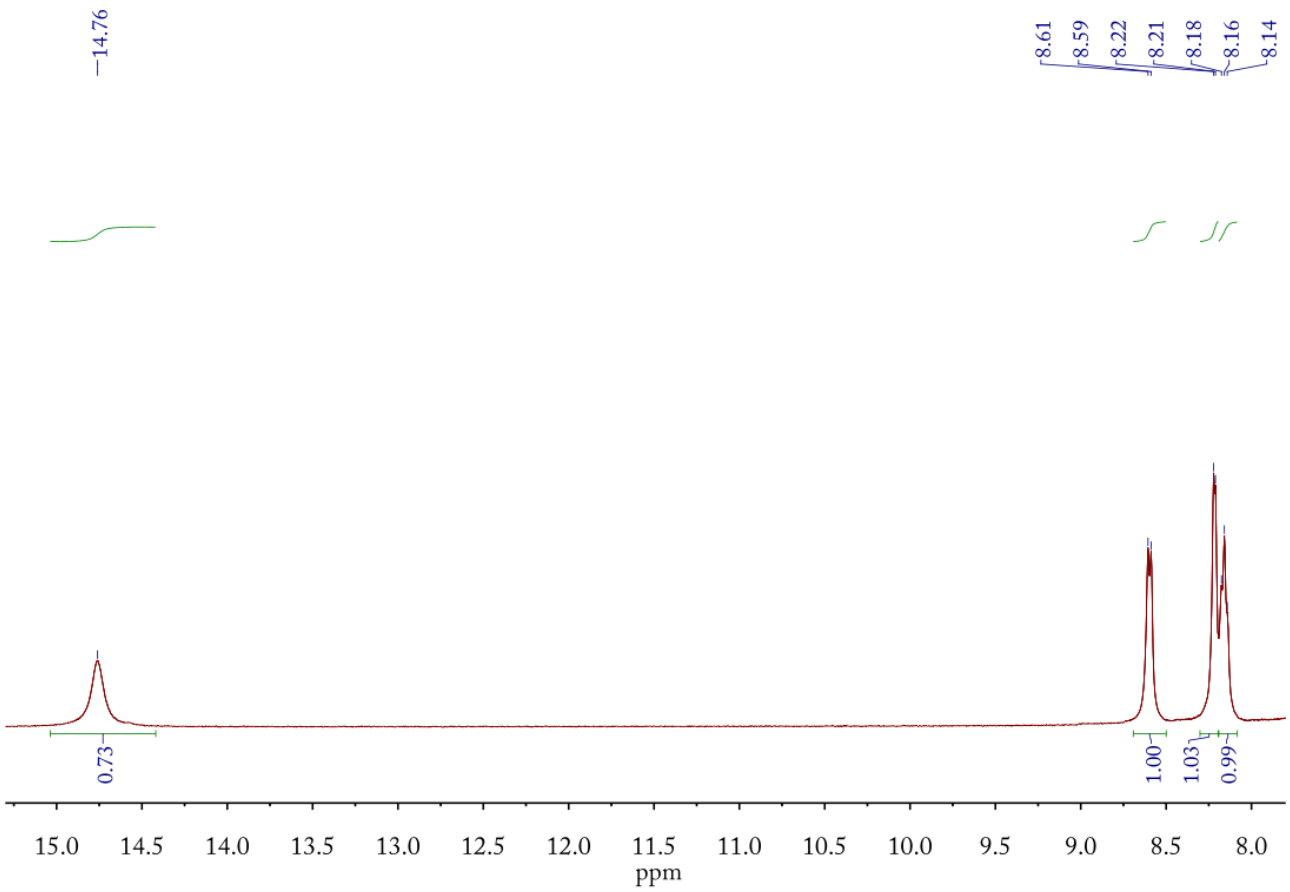

Fig. S17 ^{1}H NMR spectra of **1** in CD_2Cl_2 at 228 K

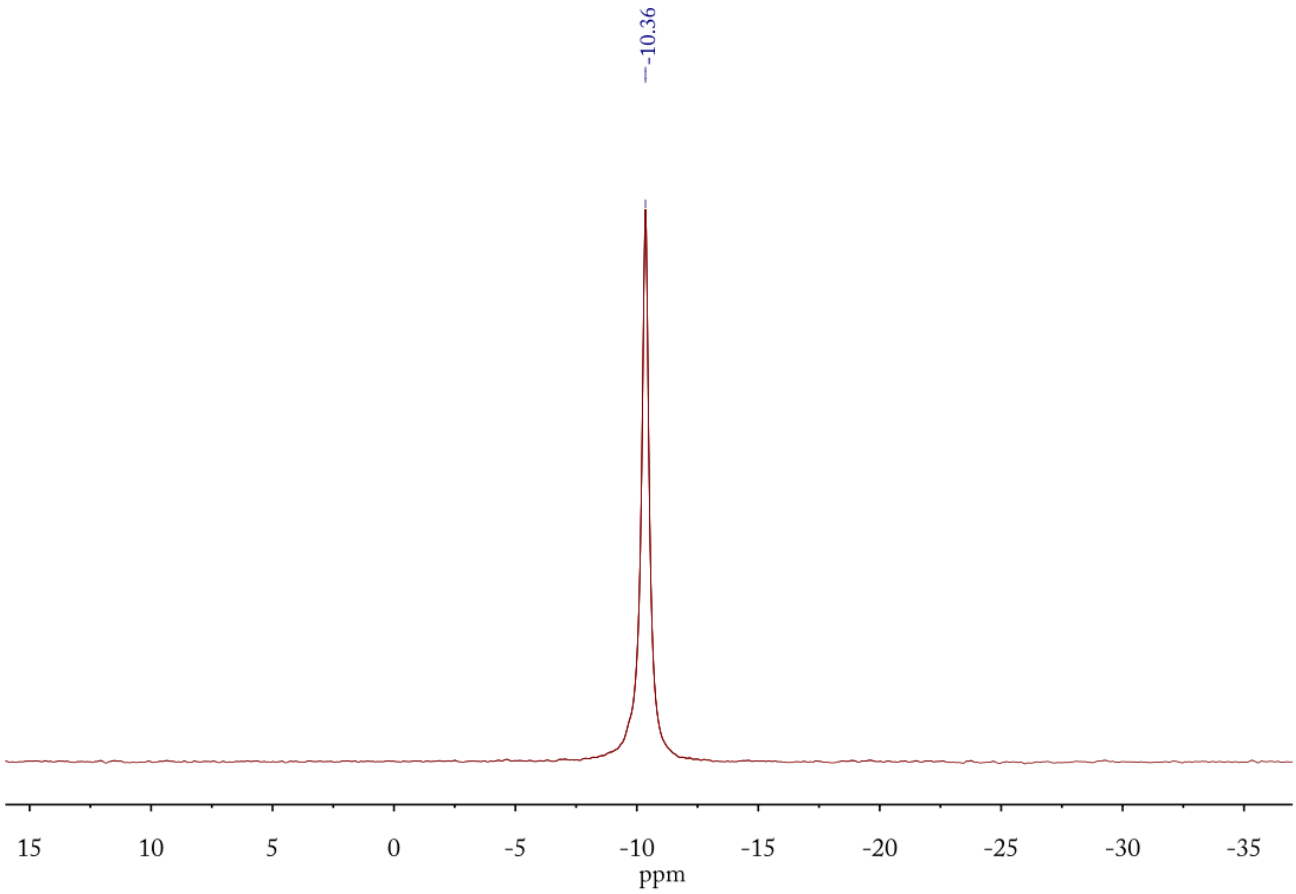

Fig. S18 ^{31}P NMR spectra of **1** in CD_2Cl_2 at 228K

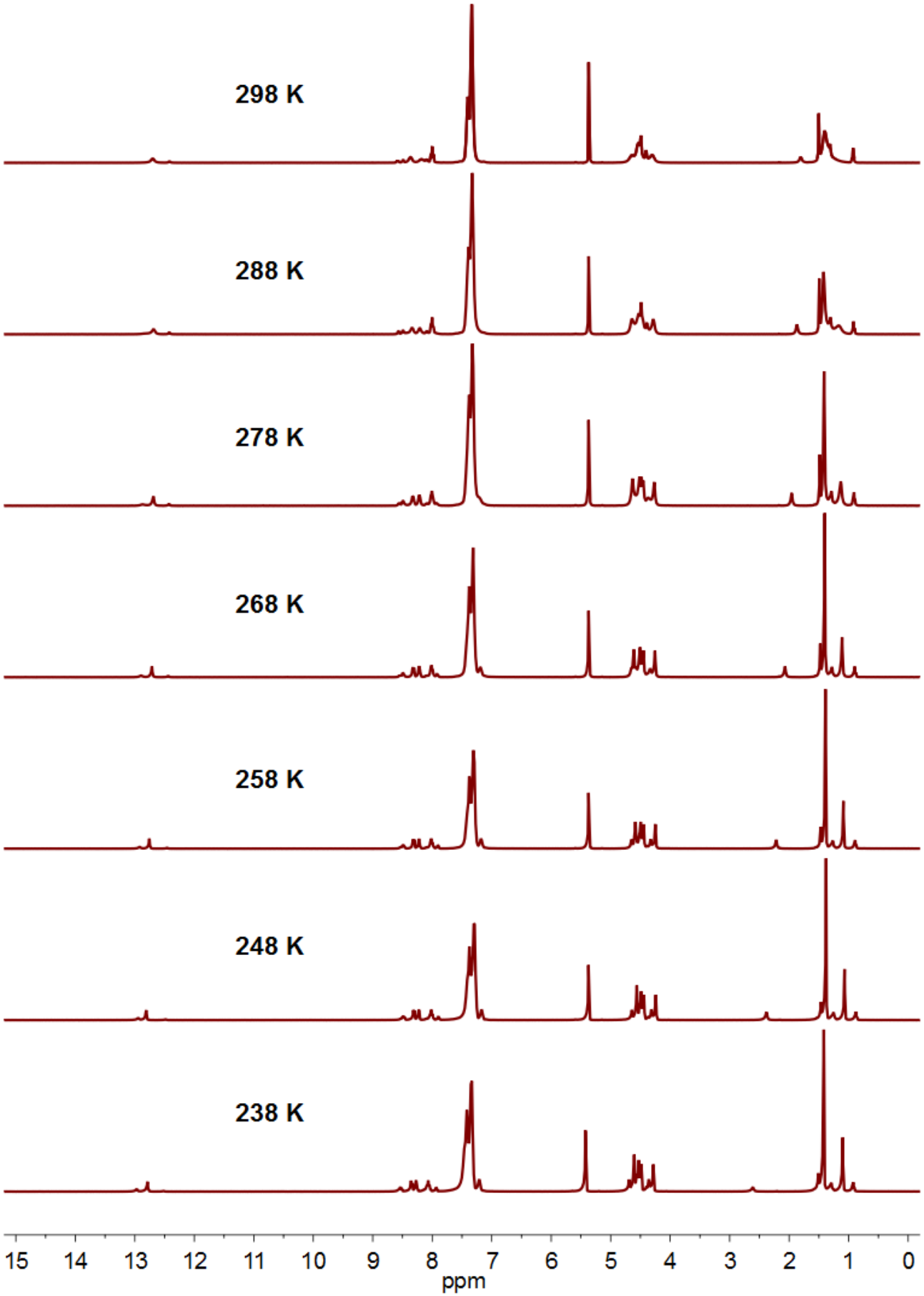
298 K
288 K
278 K
268 K
258 K
248 K
238 K
15
14
13
12
11
10
9
8
7
6
5
4
3
2
1
0
ppm

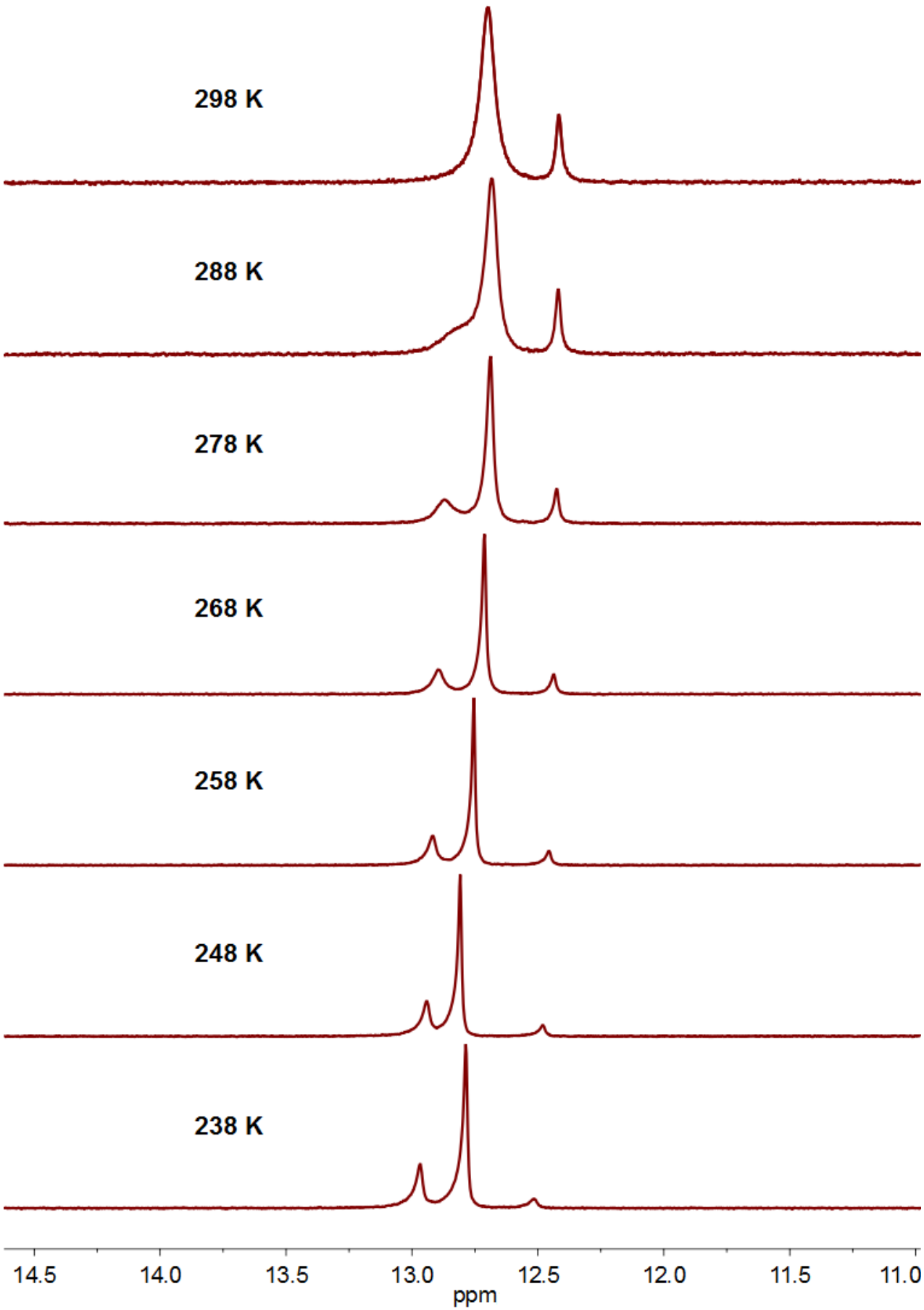

Fig. S19 Variable-temperature ^{1}H NMR spectra of **7** in CD_2Cl_2 from 298 K to 238 K

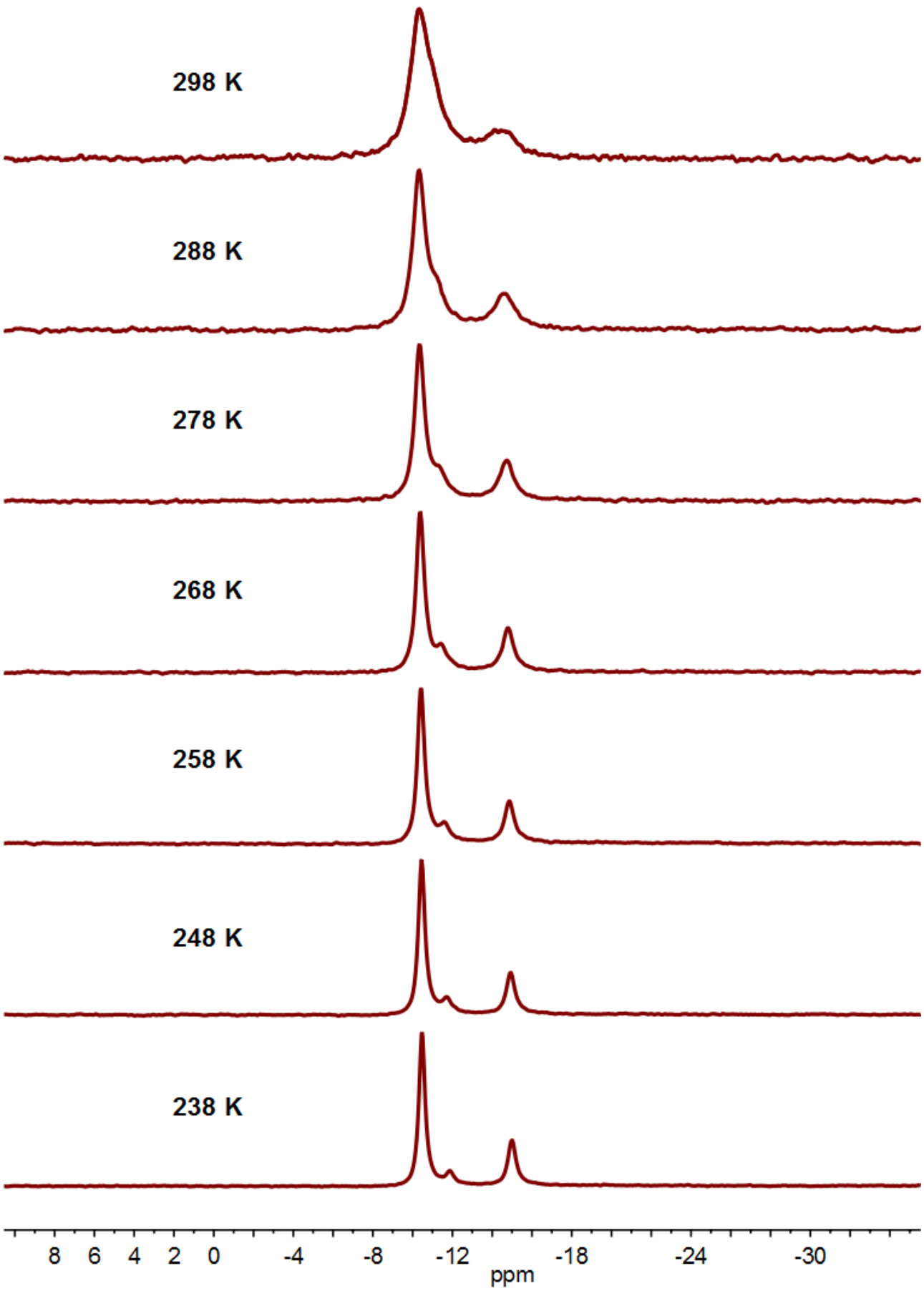

Fig. S20 Variable-temperature ^{31}P NMR spectra of **7** in CD_2Cl_2 from 298 K to 238 K

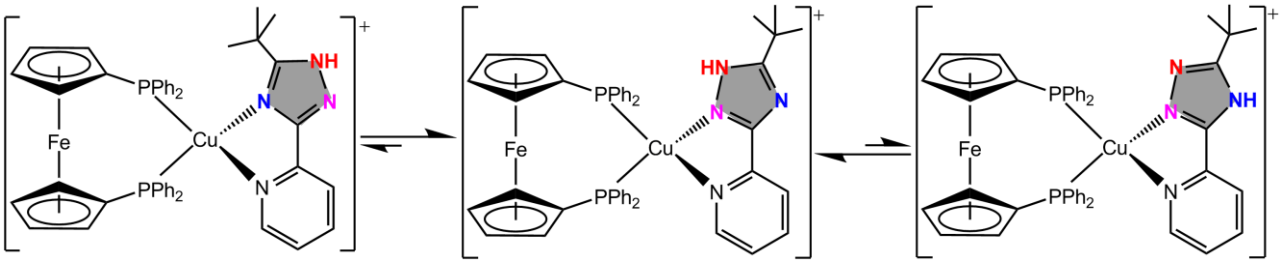

Fig. S21 Possible structures and dynamic exchange of three different isomers of **7** in CH_2Cl_2

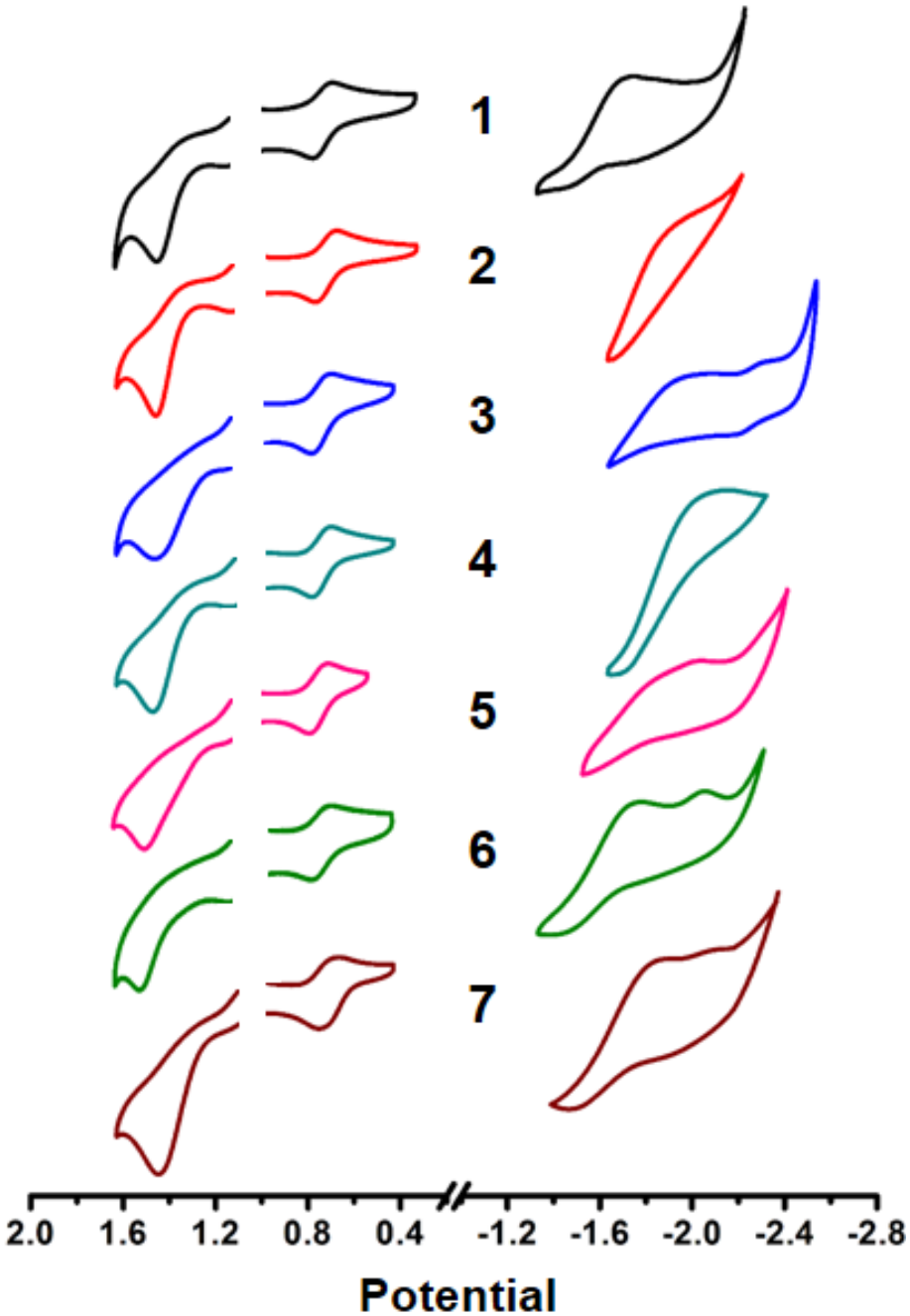

Fig. S22 Cyclic voltammograms of **1**−**7** in dry CH_2Cl_2 or THF containing 0.1 M ($^tBu_4N)PF_6$ ($Fc^{+/0}$ = 0.51 V). The scan rate of CV is 50 mV s^{-1}.

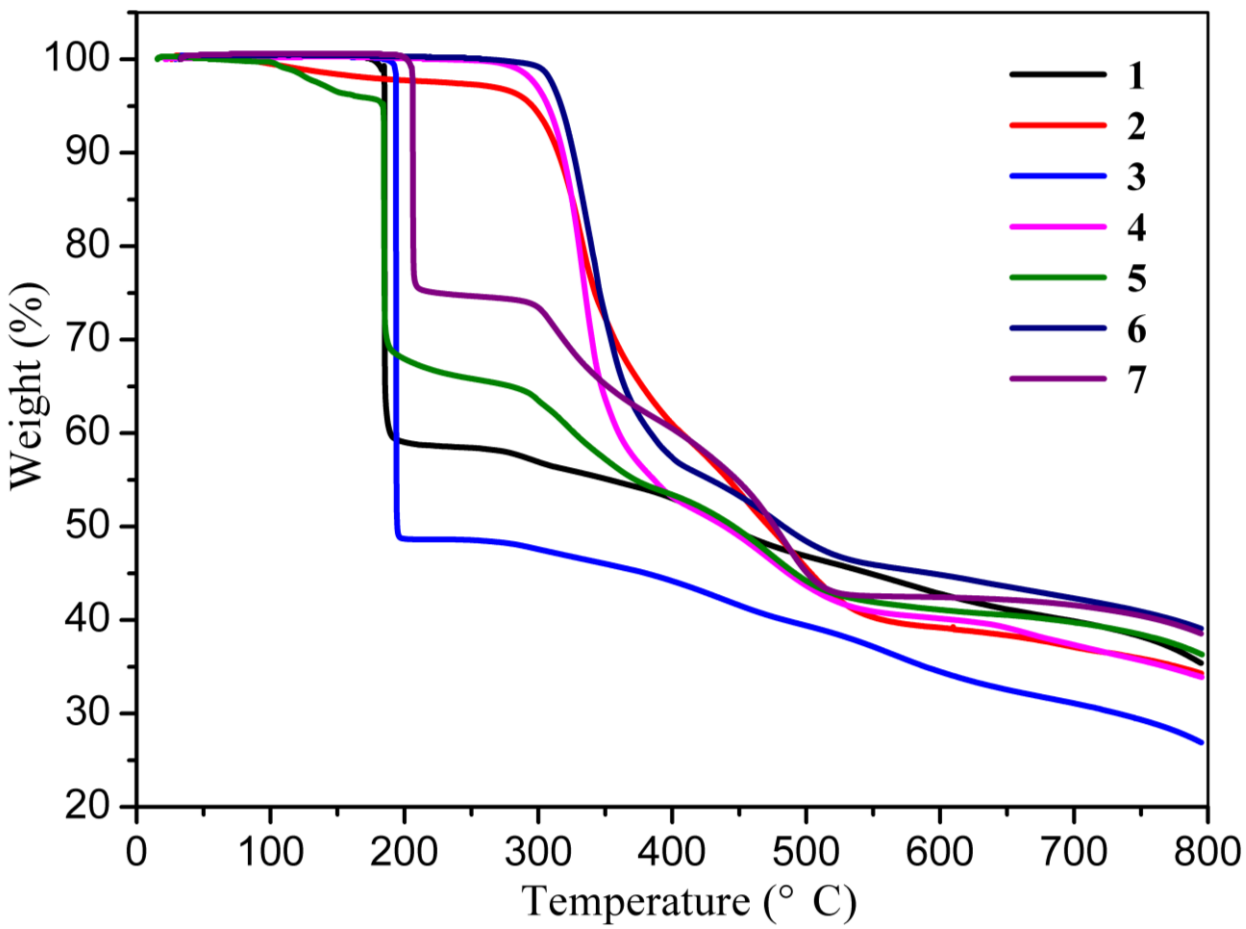

Fig. S23 TGA curves of **1**−**7** in N_2

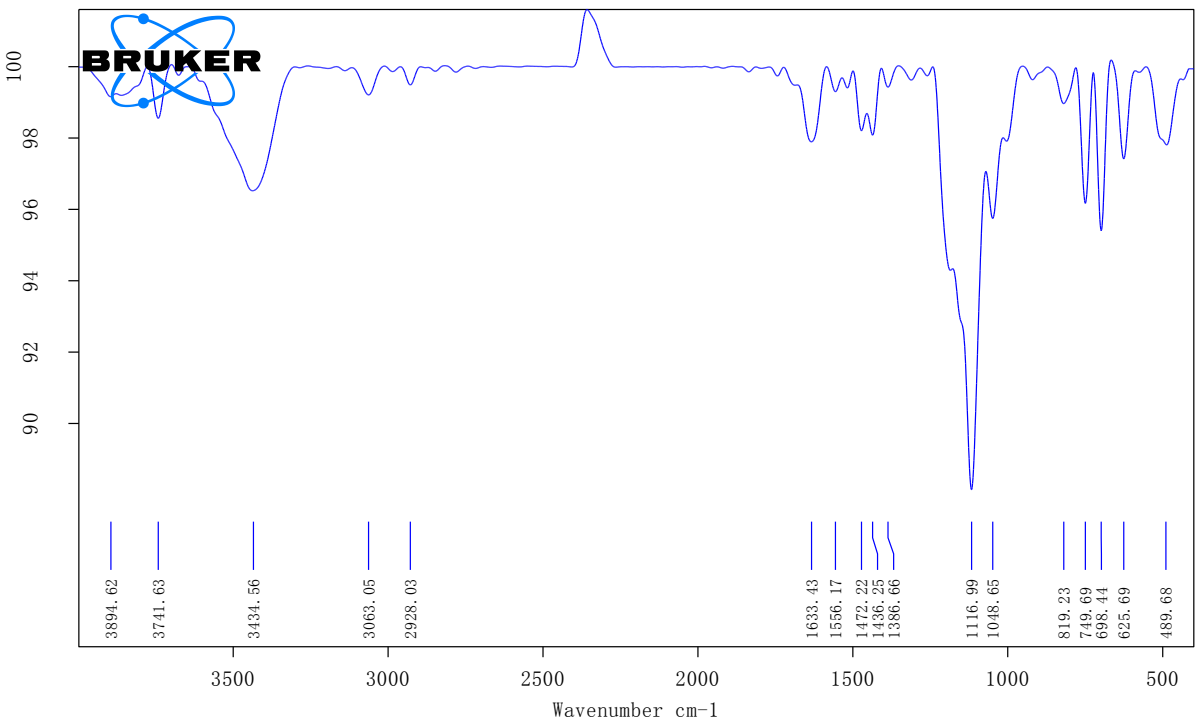

Fig. S24 IR spectrum of **1**

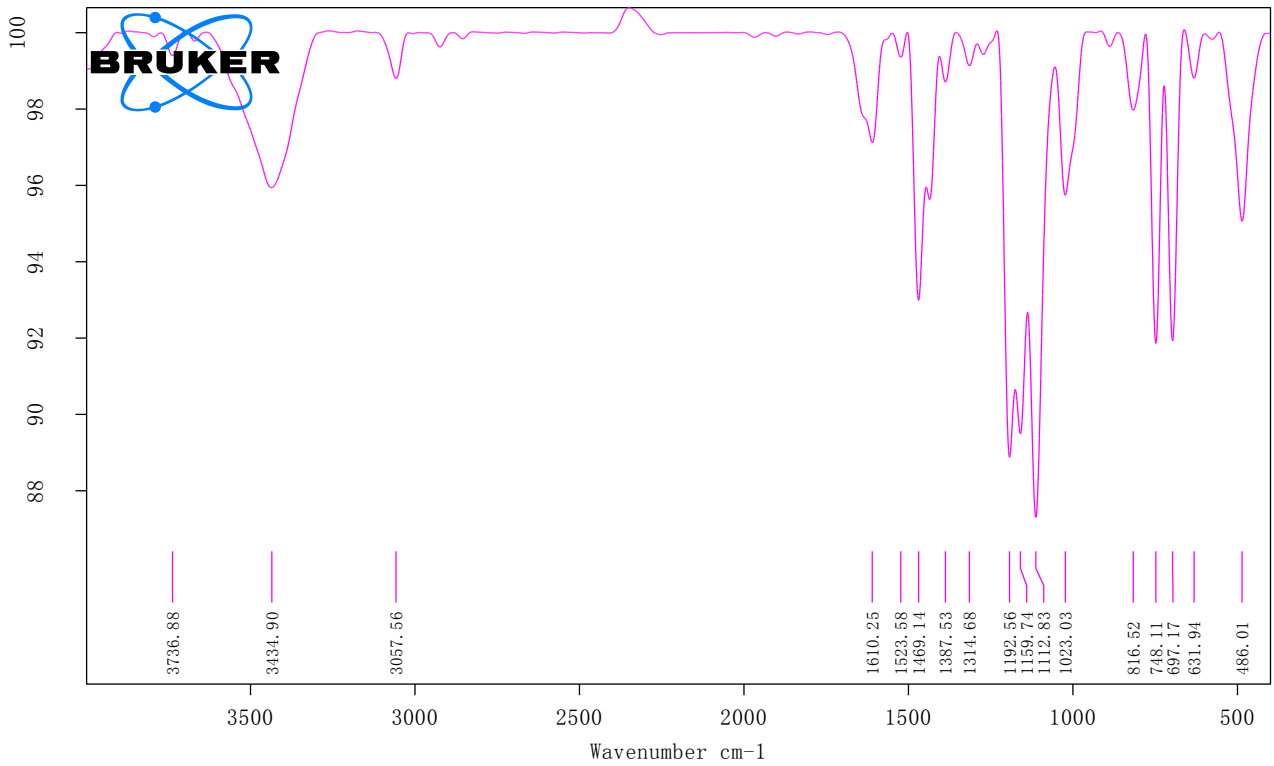

Fig. S25 IR spectrum of **2**

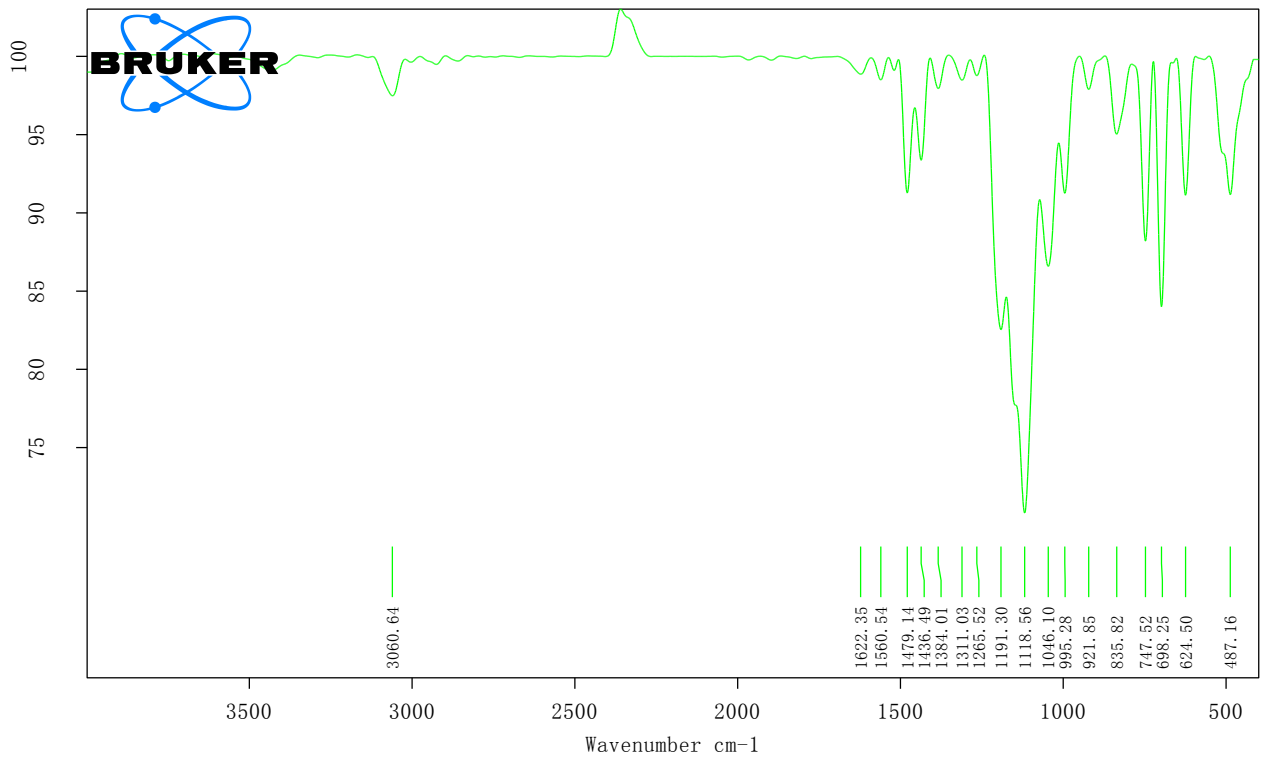

Fig. S26 IR spectrum of **3**

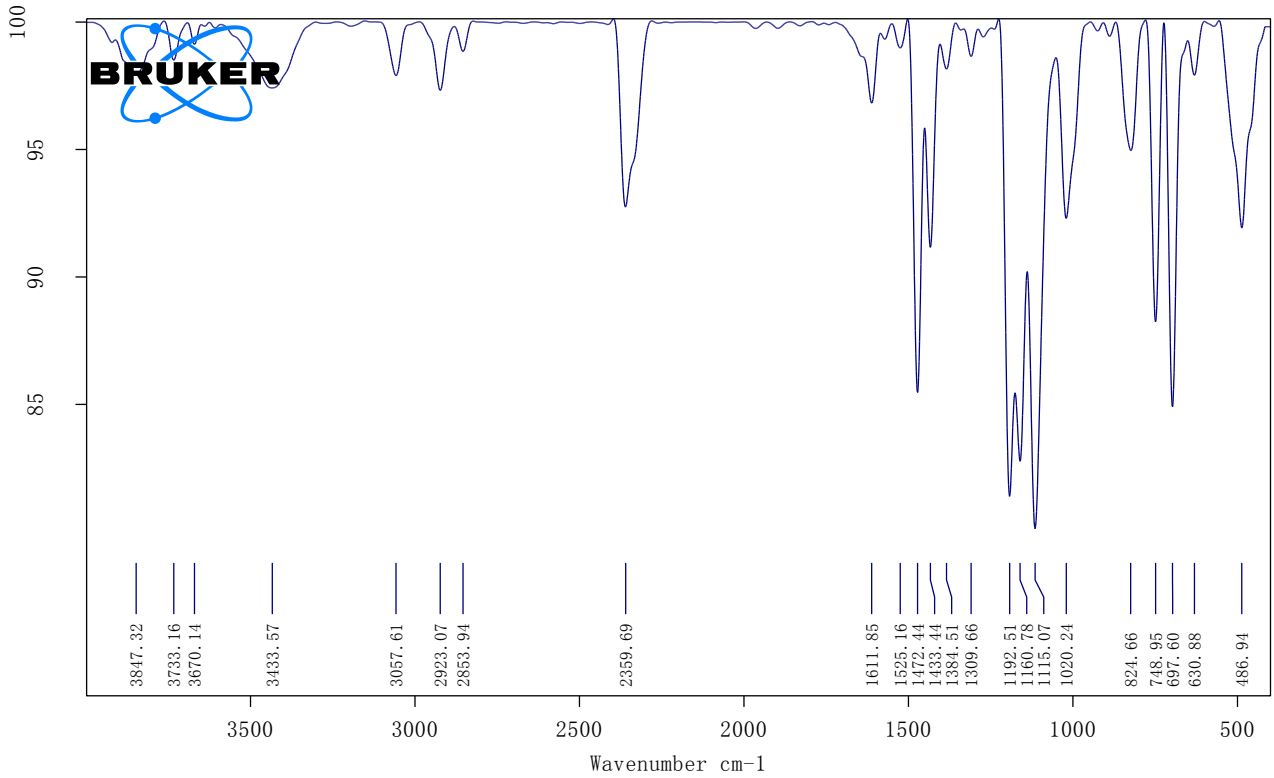

Fig. S27 IR spectrum of **4**

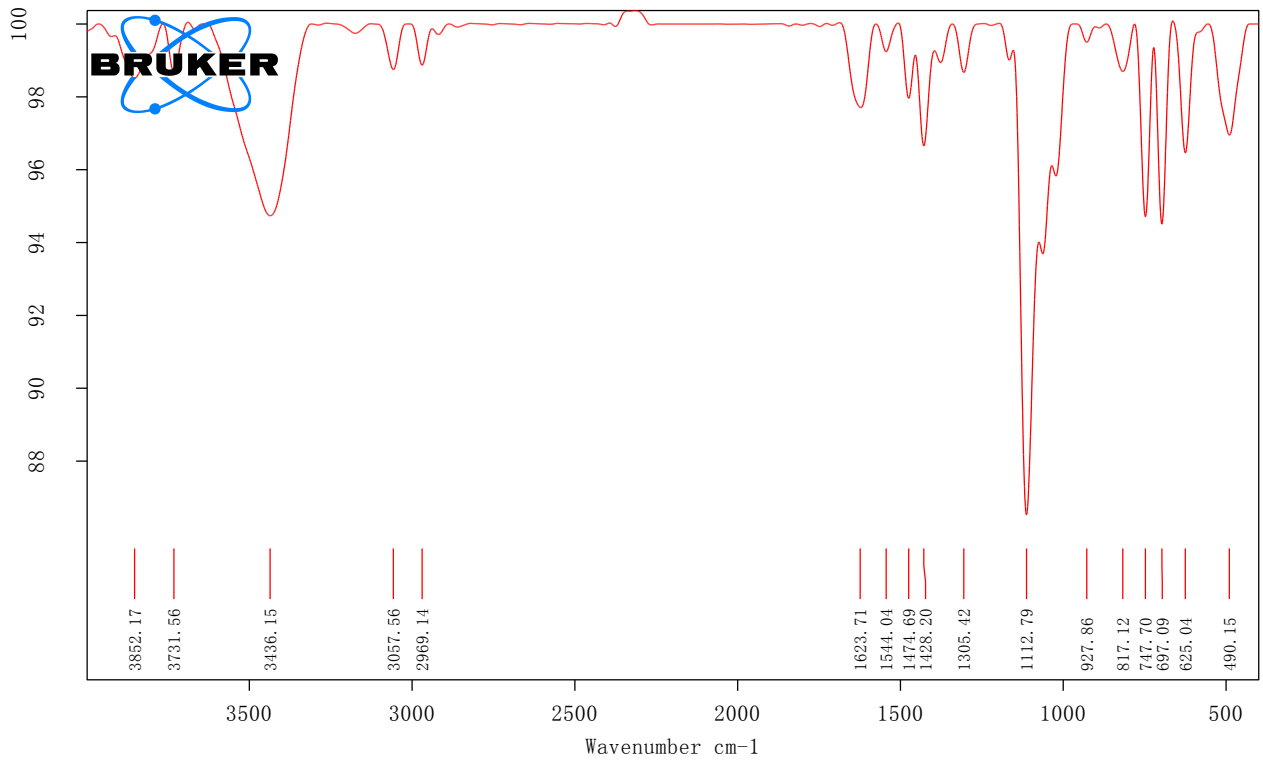

Fig. S28 IR spectrum of **5**

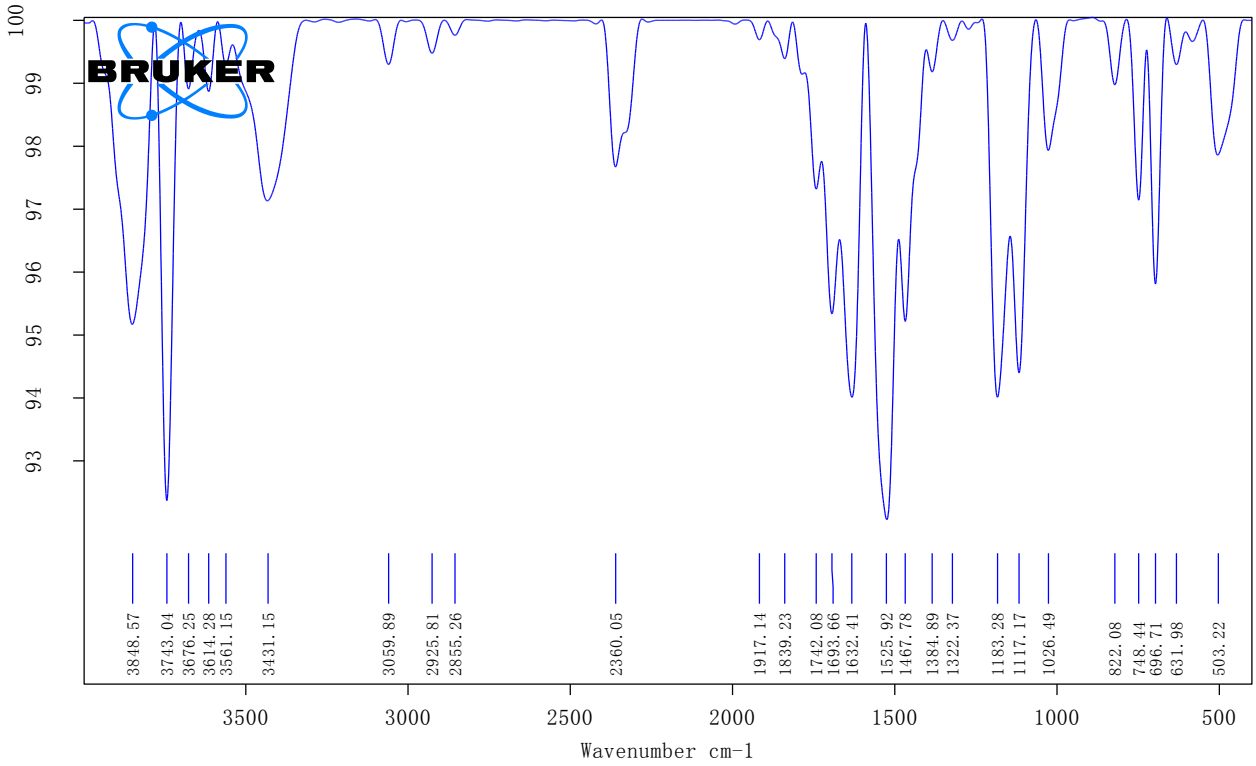

Fig. S29 IR spectrum of **6**

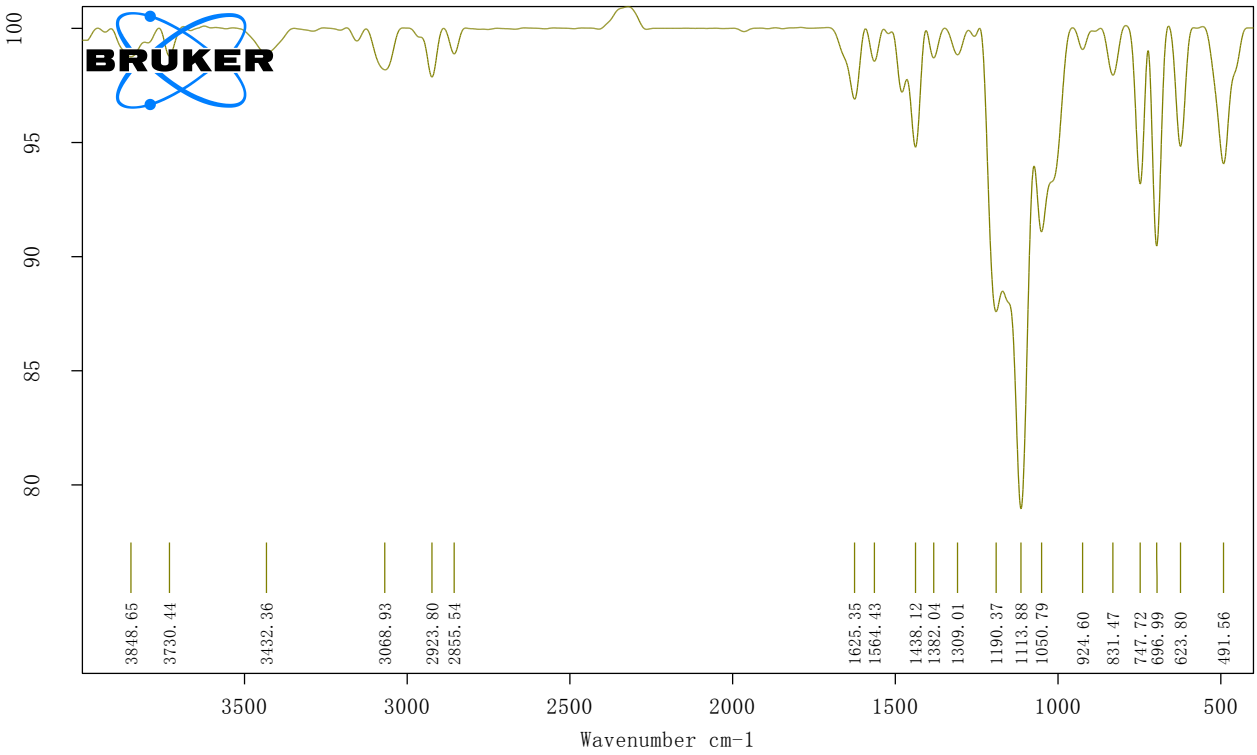

Fig. S30 IR spectrum of **7**

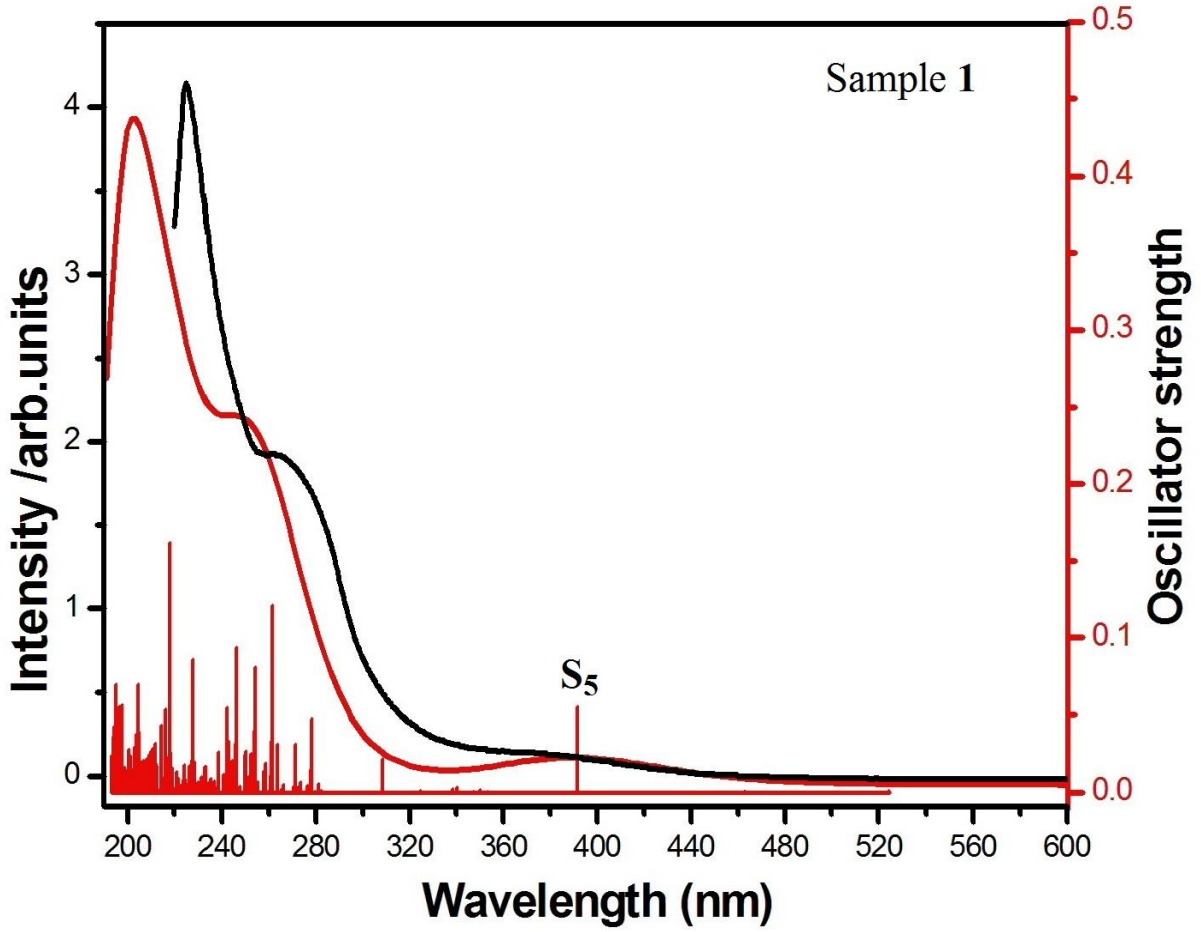
Sample 1
S5
Intensity /arb.units
Oscillator strength
Wavelength (nm)
0
1
2
3
4
0.0
0.1
0.2
0.3
0.4
0.5
200
240
280
320
360
400
440
480
520
560
600

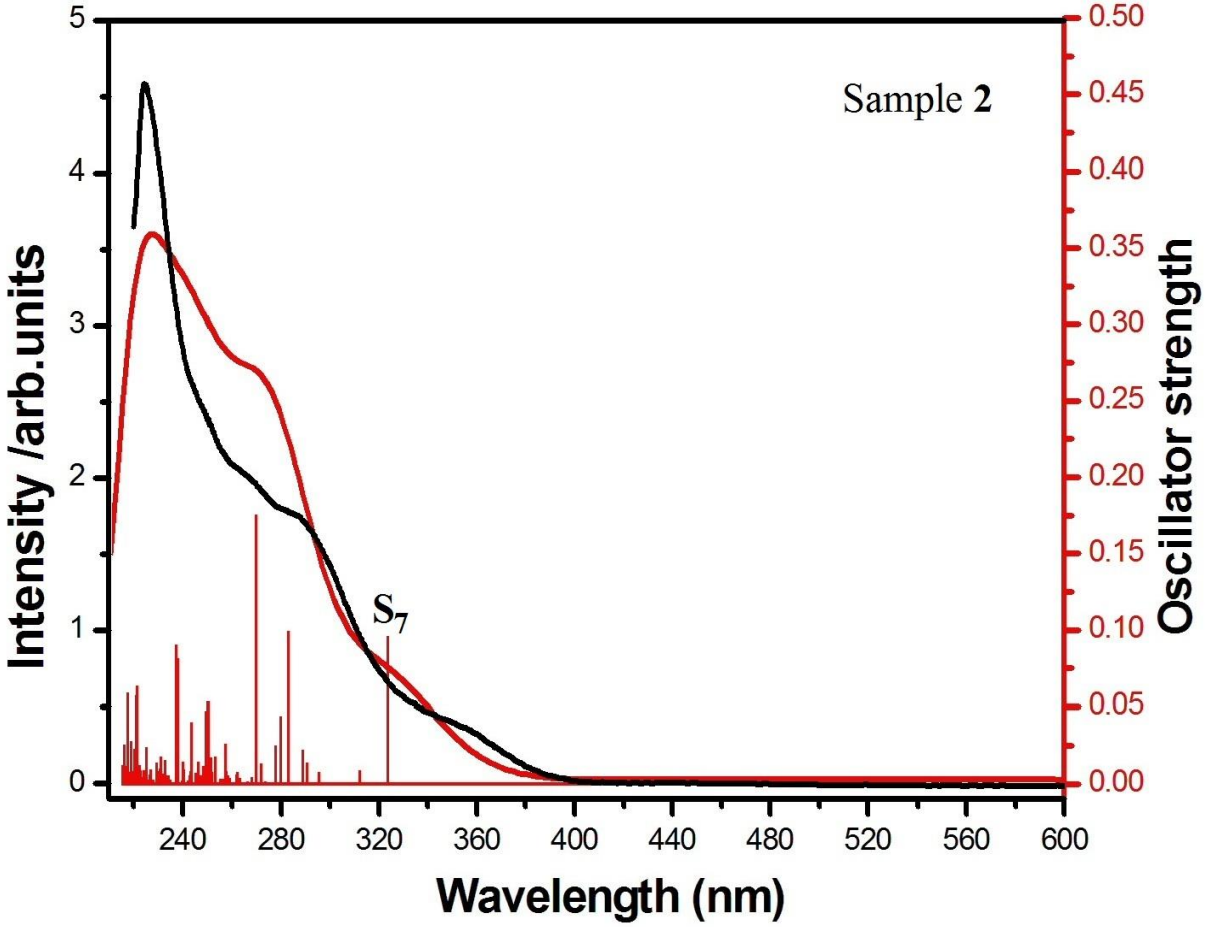
Sample 2
S7
Intensity /arb.units
Oscillator strength
Wavelength (nm)
0
1
2
3
4
5
0.00
0.05
0.10
0.15
0.20
0.25
0.30
0.35
0.40
0.45
0.50
240
280
320
360
400
440
480
520
560
600

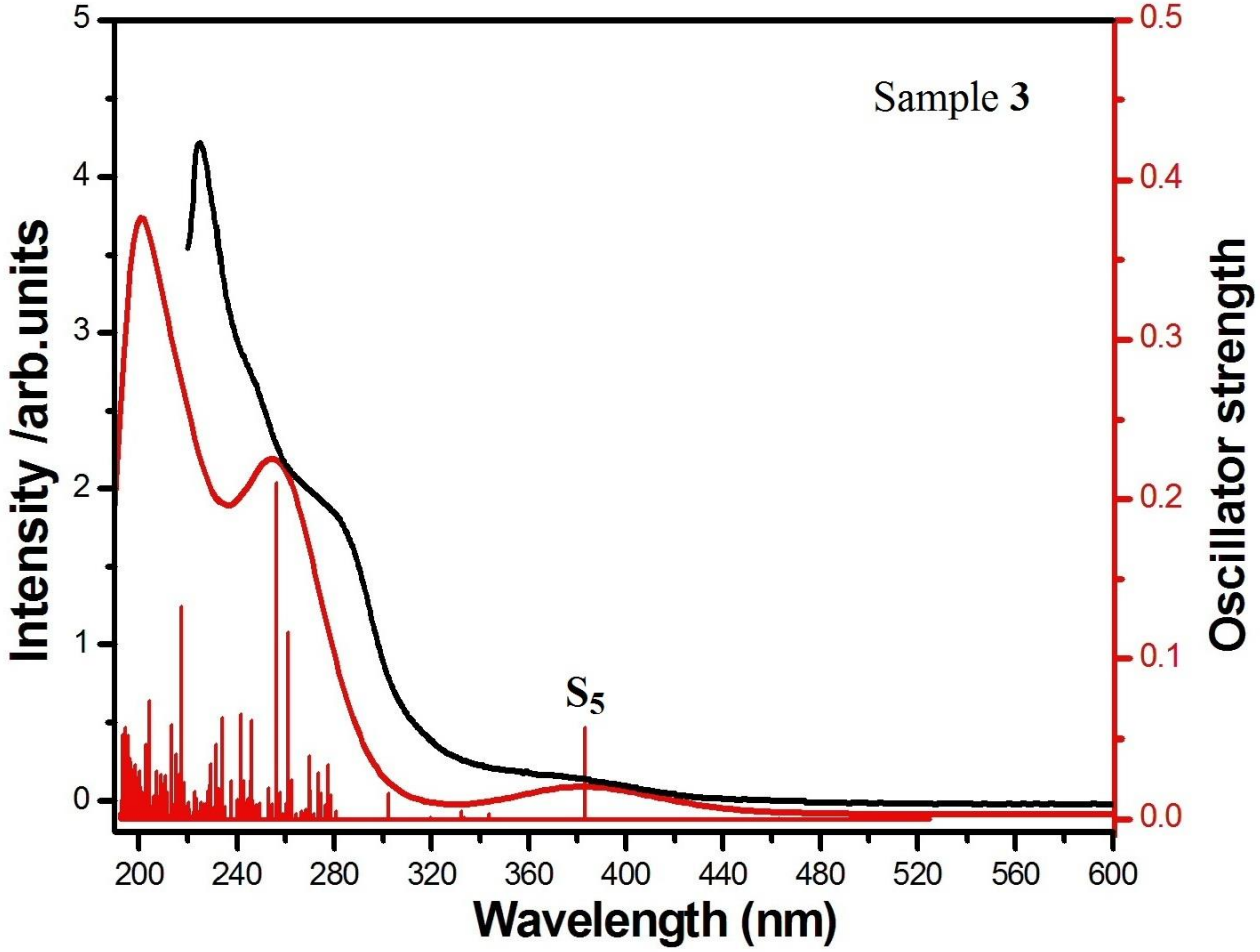
Sample 3
S5
Intensity /arb.units
Oscillator strength
Wavelength (nm)
0
1
2
3
4
5
0.0
0.1
0.2
0.3
0.4
0.5
200
240
280
320
360
400
440
480
520
560
600

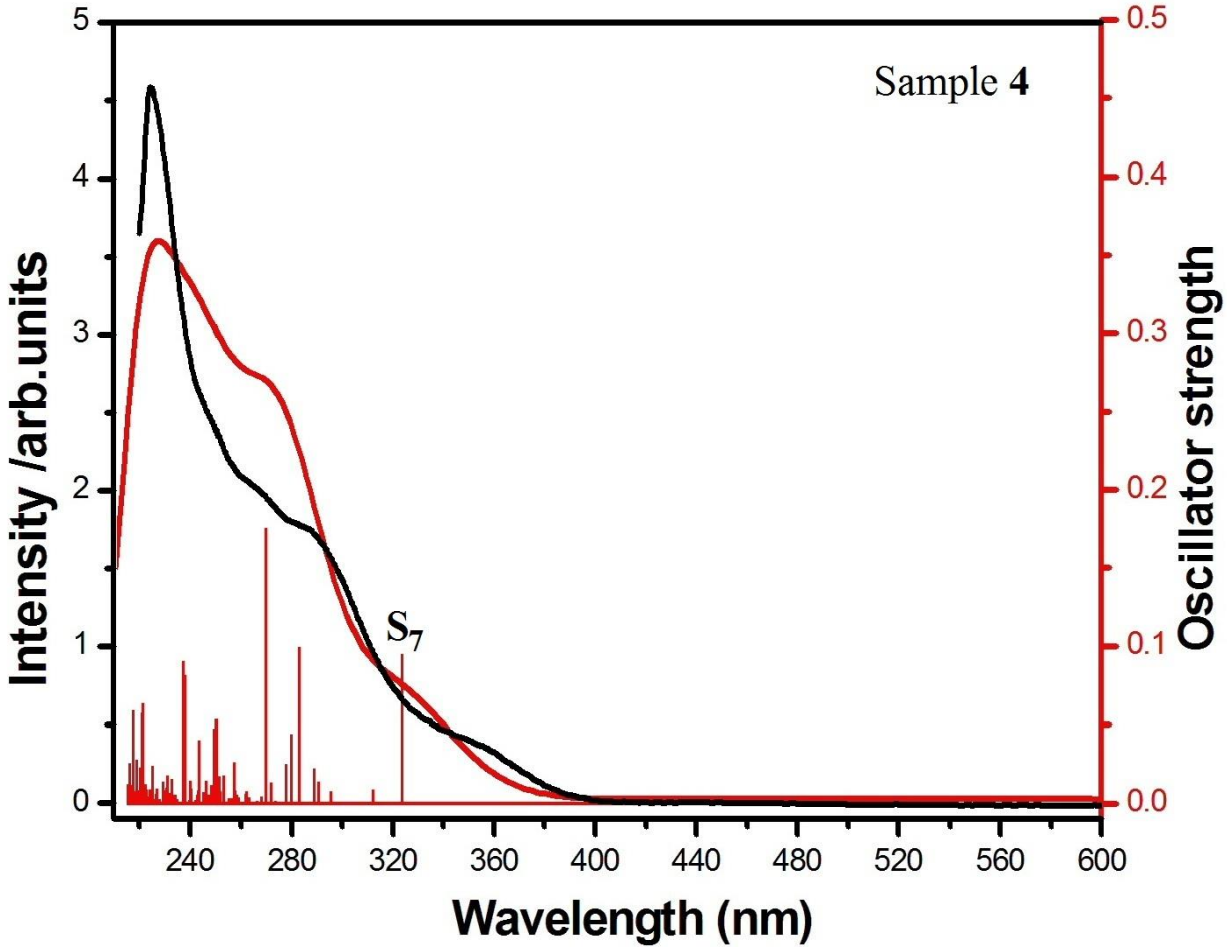
Sample 4
S7
Intensity /arb.units
Oscillator strength
Wavelength (nm)
0
1
2
3
4
5
0.0
0.1
0.2
0.3
0.4
0.5
240
280
320
360
400
440
480
520
560
600

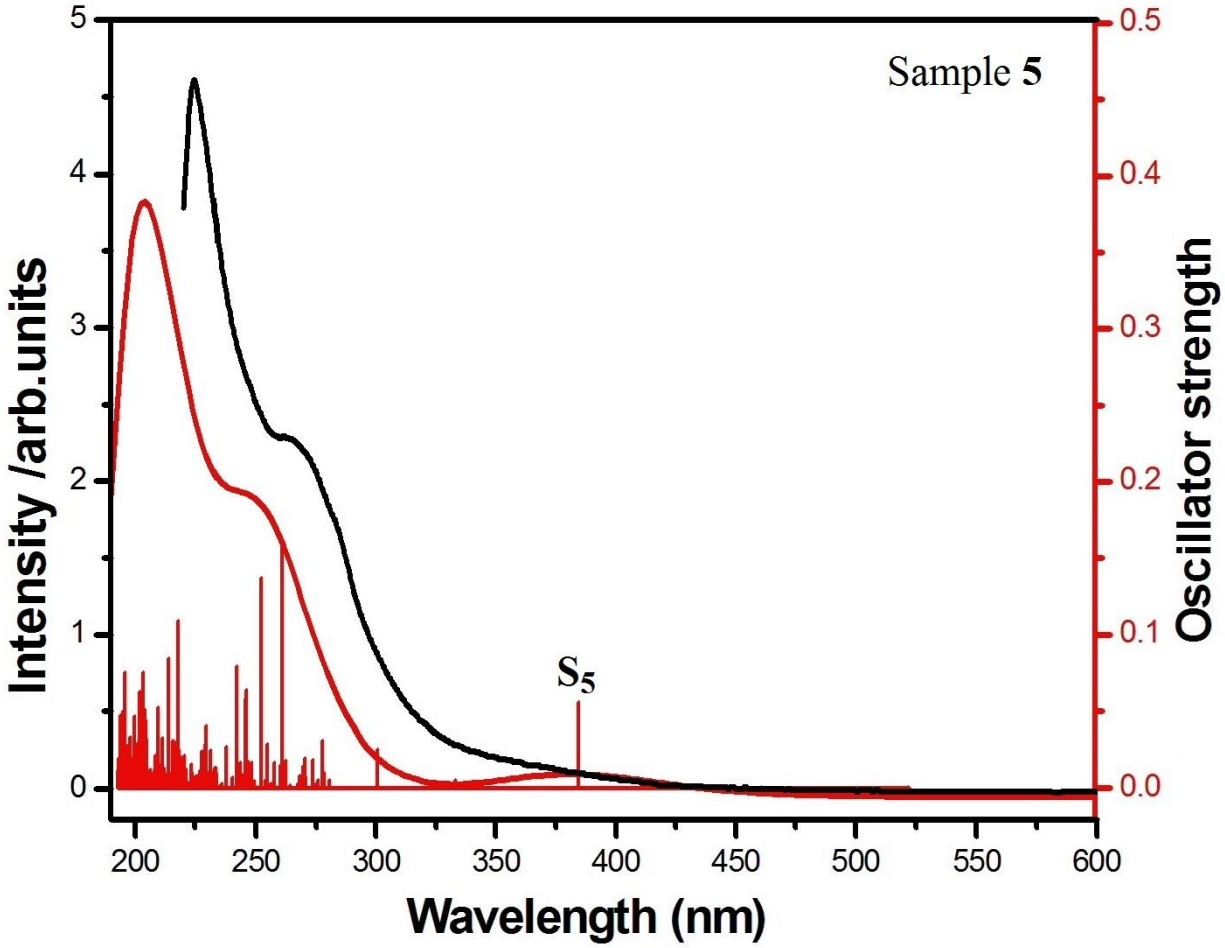
Sample 5
S5
Intensity /arb.units
Oscillator strength
Wavelength (nm)
0
1
2
3
4
5
0.0
0.1
0.2
0.3
0.4
0.5
200
250
300
350
400
450
500
550
600

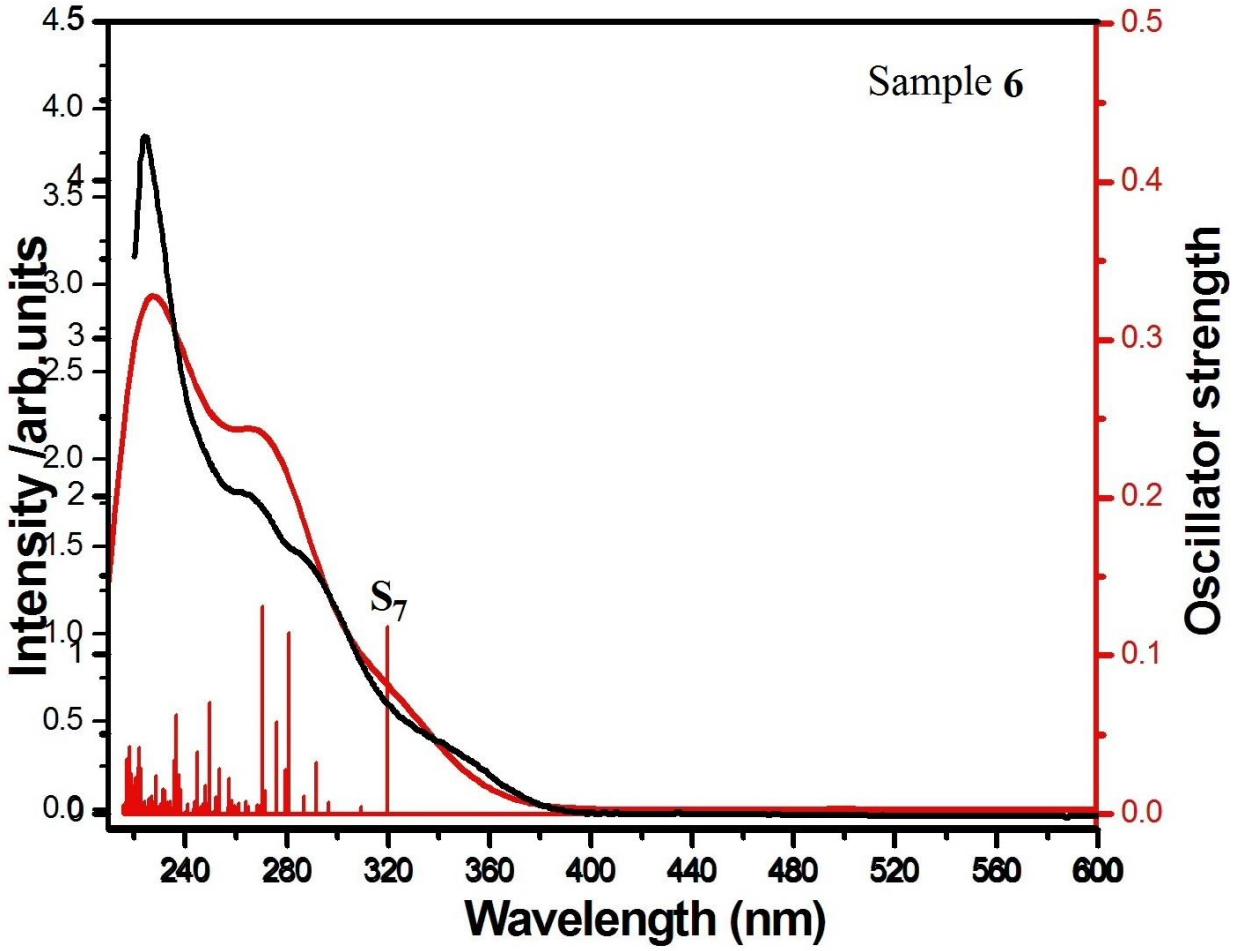
Sample 6
S7
Intensity /arb.units
Oscillator strength
Wavelength (nm)
0.0
0.5
1
1.5
2
2.5
3
3.5
4
4.0
4.5
0.0
0.1
0.2
0.3
0.4
0.5
240
280
320
360
400
440
480
520
560
600

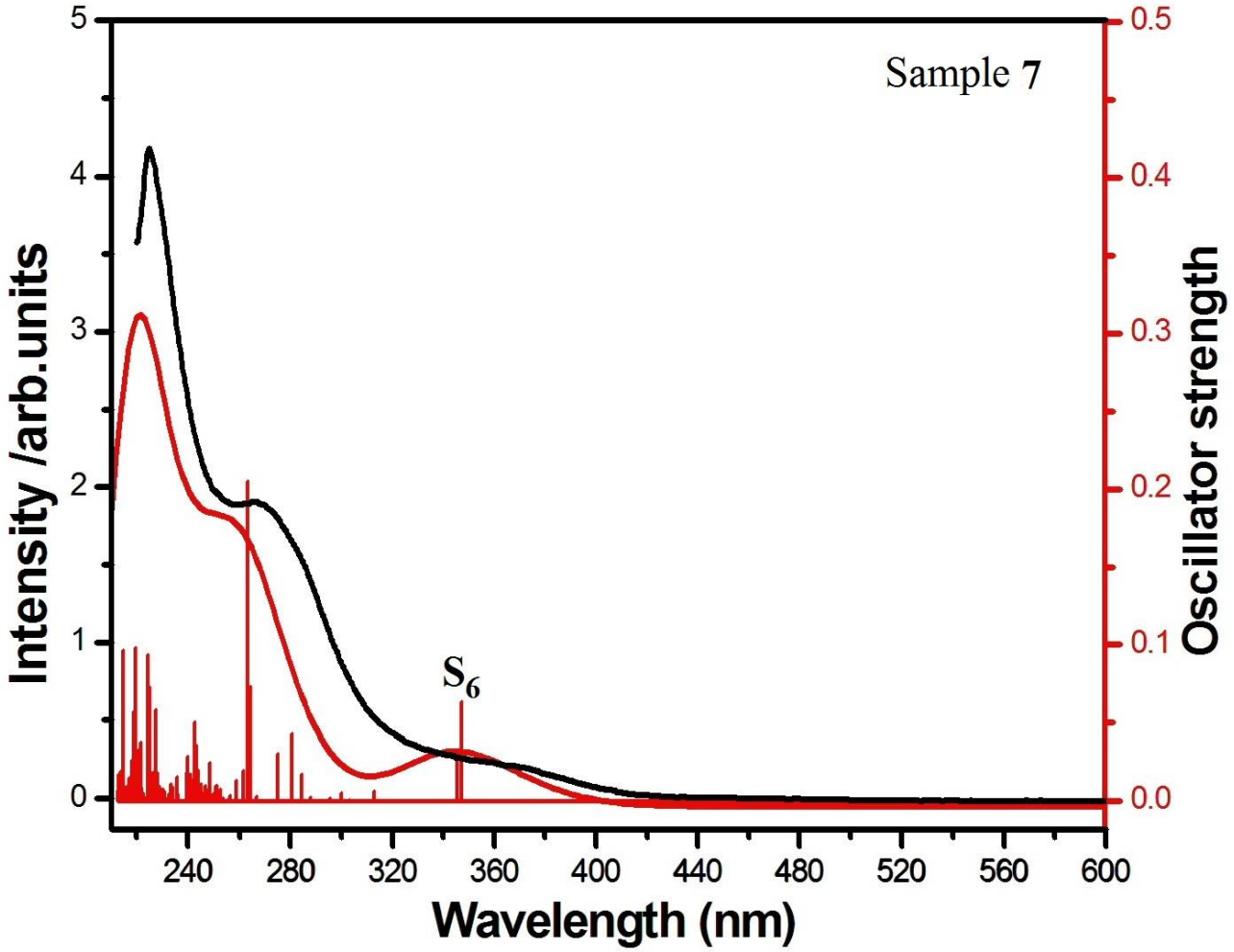

Fig. S31 Comparison of the calculated (red line) and experimental (black line) absorption spectra in CH_2Cl_2 media for **1**−**7**. Red vertical lines correspond to oscillator strength of calculated singlet-singlet transitions.

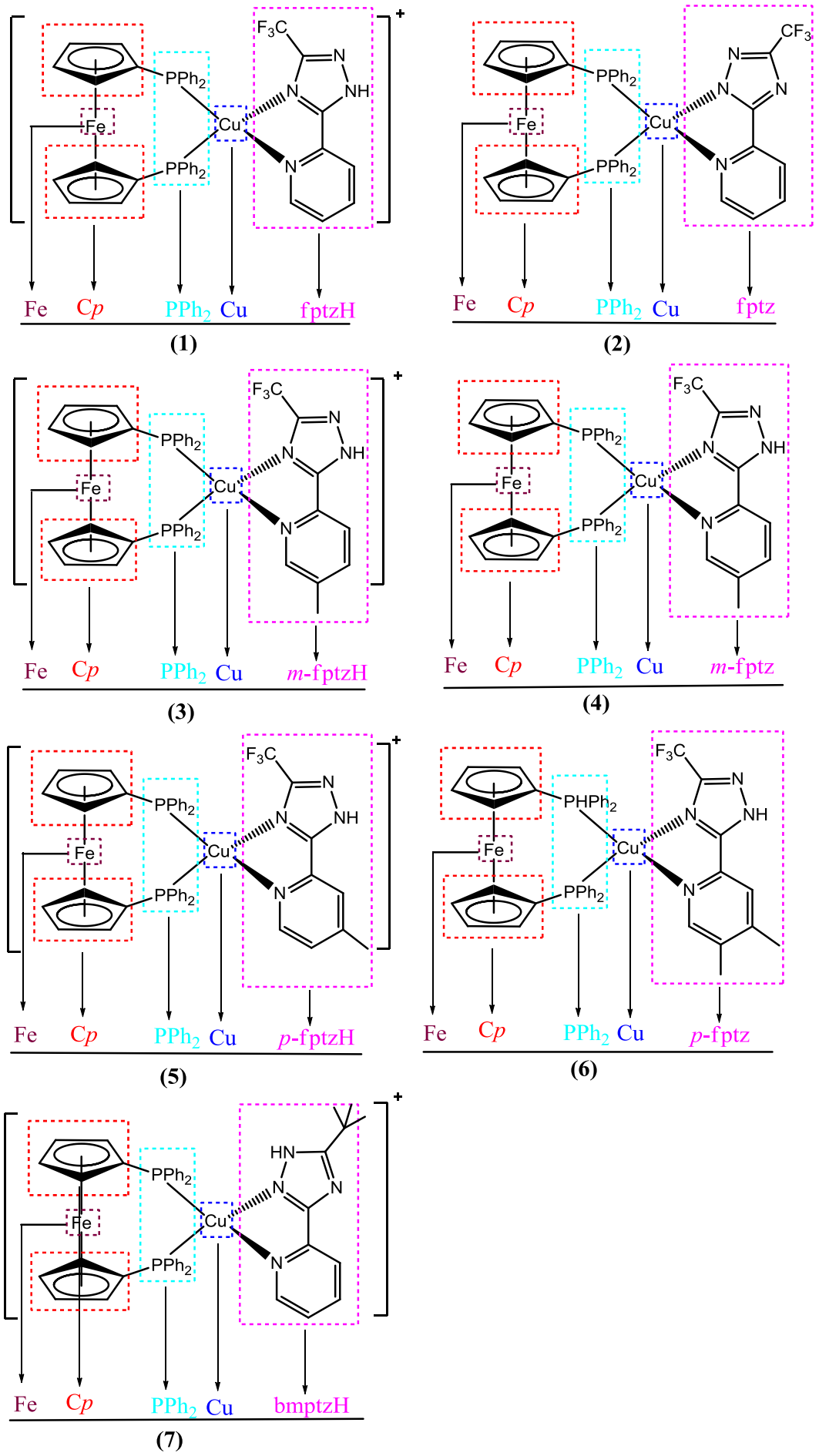

Fig. S32 Assignment of molecular fragments for **1**–**7**

Table S1 Molecular orbital compositions (%) for **1** in CH_2Cl_2 media at PBE1PBE/6-31G**/LANL2DZ level

Orbital	Main bond type	Contribution (%)				
		Fe	Cp	PPh_2	Cu	fptzH
LUMO+10	π*(PPh_2)	6.49	9.04	67.8	4.77	11.9
LUMO+8	π*(PPh_2)	9.07	11.8	65.8	8.65	4.69
LUMO	π*(fptzH)	0.43	0.0001	2.59	1.70	95.3
HOMO	d(Fe)+d(Cu)+π(PPh_2)	33.0	11.6	33.0	20.5	1.91
HOMO-1	d(Fe)	77.1	19.5	2.37	0.80	0.19
HOMO-2	d(Fe)+d(Cu)	48.4	12.7	22.5	14.3	1.08

Table S2 Molecular orbital compositions (%) for **2** in CH_2Cl_2 media at PBE1PBE/6-31G**/LANL2DZ level

Orbital	Main bond type	Contribution (%)				
		Fe	Cp	PPh_2	Cu	fptz
LUMO+8	π*(PPh_2)	15.0	15.4	61.5	4.00	2.40
LUMO+7	π*(PPh_2)	22.9	17.2	53.4	3.27	1.89
LUMO+6	d(Fe)+π*(PPh_2)+π*(Cp)	33.9	22.3	38.0	3.02	0.67
LUMO	π*(fptz)	0.46	0.67	5.02	5.29	88.4
HOMO	d(Cu)+π(PPh_2)	12.2	6.20	39.8	32.6	8.50
HOMO-1	d(Fe)	69.8	18.9	4.20	4.96	2.00
HOMO-2	d(Fe)	65.8	7.30	4.48	4.86	7.38

Table S3 Molecular orbital compositions (%) for **3** in CH_2Cl_2 media at PBE1PBE/6-31G**/LANL2DZ level

Orbital	Main bond type	Contribution (%)				
		Fe	Cp	PPh_2	Cu	*m*-fptzH
LUMO+10	d(Fe)+π*(PPh_2)+π*(Cp)	32.8	24.3	38.1	3.71	1.08
LUMO+8	d(Fe)+π*(PPh_2)+π*(Cp)	35.2	21.3	22.8	4.67	16.1
LUMO	π*(*m*-fptzH)	0.09	0.48	2.68	1.71	95.1
HOMO	d(Fe)+d(Cu)+ π(PPh_2)	32.3	11.5	33.0	21.0	2.13
HOMO-1	d(Fe)+π(Cp)	77.1	25.5	2.38	0.83	0.20
HOMO-2	d(Fe)+π(PPh_2)	49.0	13.8	21.8	14.2	1.19

Table S4 Molecular orbital compositions (%) for **4** in CH_2Cl_2 media at PBE1PBE/6-31G**/LANL2DZ level

Orbital	Main bond type	Contribution (%)				
		Fe	Cp	PPh_2	Cu	*m*-fptz
LUMO+8	π*(PPh_2)	13.6	14.5	64.9	4.18	2.83
LUMO+7	π*(PPh_2)	24.8	17.7	51.3	3.45	2.76
LUMO+6	d(Fe)+π*(PPh_2)	33.0	21.8	41.5	3.03	0.62
LUMO	π*(*m*-fptz)	0.53	0.70	5.19	5.11	88.5
HOMO	d(Cu)+π(PPh_2)	11.6	10.7	40.1	32.7	21.1
HOMO-1	d(Fe)	68.7	18.8	4.56	5.65	2.31
HOMO-2	d(Fe)	57.7	15.1	2.40	3.23	21.6

Table S5 Molecular orbital compositions (%) for **5** in CH_2Cl_2 media at PBE1PBE/6-31G**/LANL2DZ level

Orbital	Main bond type	Contribution (%)				
		Fe	Cp	PPh_2	Cu	*p*-fptzH
LUMO+10	π*(PPh_2)	30.2	22.7	41.7	4.29	1.11
LUMO+8	d(Fe)+π*(PPh_2)+π*(Cp)	35.5	21.9	25.9	5.36	11.4
LUMO	π*(*p*-fptzH)	0.07	0.37	2.50	1.54	95.5
HOMO	d(Fe)+d(Cu)+ π(PPh_2)	32.0	11.5	32.9	21.4	2.21
HOMO-1	d(Fe)	77.2	19.6	2.27	0.78	0.18
HOMO-2	d(Fe)	49.1	13.9	21.3	14.5	1.25

Table S6 Molecular orbital compositions (%) for **6** in CH_2Cl_2 media at PBE1PBE/6-31G**/LANL2DZ level

Orbital	Main bond type	Contribution (%)				
		Fe	Cp	PPh_2	Cu	*p*-fptz
LUMO+8	π*(PPh_2)	22.1	18.0	53.6	4.14	2.08
LUMO+7	π*(PPh_2)	23.4	15.8	53.2	4.50	3.04
LUMO+6	π*(PPh_2)	21.1	17.6	57.6	2.77	0.89
LUMO	π*(*p*-fptz)	0.52	0.68	25.9	4.92	67.9
HOMO	d(Cu)+π(PPh_2)	12.0	6.20	41.1	32.9	7.83
HOMO-1	d(Fe)	68.8	18.7	4.71	5.58	2.21
HOMO-2	d(Fe)	65.8	17.3	4.77	4.95	7.19

Table S7 Molecular orbital compositions (%) for **7** in CH_2Cl_2 media at PBE1PBE/6-31G**/LANL2DZ level

Orbital	Main bond type	Contribution (%)				
		Fe	Cp	PPh_2	Cu	*p*-fptz
LUMO+9	d(Fe)+π*(PPh_2)+π*(Cp)	29.9	22.7	43.7	2.93	0.73
LUMO+7	d(Fe)+π*(PPh_2)+π*(Cp)	44.4	26.4	23.4	4.51	1.27
LUMO	π*(*p*-fptz)	0.25	0.47	4.13	4.25	90.9
HOMO	d(Fe)+d(Cu)+π(PPh_2)	24.3	9.60	37.6	24.9	3.65
HOMO-1	d(Fe)	77.3	19.5	2.26	0.78	0.21
HOMO-2	d(Fe)	56.5	15.5	15.6	10.9	1.55